Four-body model for transfer ionization in fast ion-atom collisions

Dževad Belkić,[1] Ivan Mančev,[2] and Volker Mergel[3]
[1]*University of Stockholm, Atomic Physics, Frescativägen 24, S-104 05 Stockholm, Sweden*
[2]*University of Niš, Department of Physics, P.O. Box 91, 18001 Niš, Yugoslavia*
[3]*Institut für Kernphysik, Universität Frankfurt, D60486 Frankfurt am Main, Germany*
(Received 1 July 1996)

Total cross sections for transfer ionization in fast collisions of a bare nucleus with helium are examined in the four-body distorted-wave formalism. A special emphasis is given to a proper inclusion of *dynamic* electron-electron correlation effects. For this purpose, the four-body continuum distorted-wave (CDW-4B) approximation with the correct boundary conditions is introduced. Along with the appropriate potential operators containing a *single* electron placed on one and/or both nuclear centers, accompanied by the corresponding Coulomb waves for continuum intermediate states, the *dielectronic* interaction $V_{12}=1/r_{12}\equiv 1/|\vec{r}_1-\vec{r}_2|$ also explicitly appears in the perturbation potential of the transition probability amplitude. The inclusion of the potential V_{12} is essential for the description of the Thomas P-e-e scattering, through which one of the target electrons could be captured or ionized without ever experiencing any direct interaction with the projectile P. The total cross sections σ_{if} due to such a correlated CDW-4B theory are computed exactly and very efficiently by means of precise evaluation of certain seven-dimensional quadratures in momentum space. The proposed method is shown to be superior to the corresponding independent event model (CDW-IEM), which also proceeds through the same effort on multidimensional scattering integrals, but largely overestimates the measured values for σ_{if}. Comparisons between the present results σ_{if} and the available experimental data at $E=30-600$ keV/amu for transfer ionization in the He^{2+}-He collision yield satisfactory agreement at impact energies $E\geqslant 80$ keV/amu. This is in full harmony with the well-known low-energy limit of the validity of the CDW-3B method assessed previously for the genuine three-body charge exchange in collisions between a fully stripped projectile and a hydrogenlike atomic target. [S1050-2947(97)04801-4]

PACS number(s): 34.70.+e, 82.30.Fi

I. INTRODUCTION

In fast collisions of bare nuclei or hydrogenlike projectiles with the helium target, much attention has recently been devoted to two-electron transitions. These include double ionization (DI), excitation (DE), and capture (DC), as well as some hybrid phenomena including transfer ionization (TI) or transfer excitation (TE) in its resonant (RTE) or nonresonant (NTE) forms [1–21]. The present study is devoted to the TI process. Most of the related experimental work has thus far been concerned with total cross sections [1–6] and only a few measurements relate to angular distributions [7,8]. On the theoretical side, the majority of the methods have dealt with the independent particle model (IPM) or independent event model (IEM) [9–13]. This procedure assumes that the two electrons undergo completely independent transitions without influencing each other at all. Such an *a priori* absence of the dielectronic interaction $V_{12}=1/r_{12}$ eliminates the IPM from the list of the possible methods for studying the dynamic electron-electron correlations as undoubtedly the most challenging facet of these double transitions. Static interelectron correlations in heliumlike subsystems could partially be included in the IPM through the configuration interaction by expressing the two-electron wave function as a linear combination of single-particle orbitals. However, the obtained results are generally inadequate, since they do not compare favorably with measurements in a *consistent* manner, as best illustrated for the DC within the IPM version of the continuum distorted wave (CDW-IPM) approximation [17]. Static electron correlation effects could partially be incorporated into the TCDW-IEM (T stands for the target) via the wave function of Pluvinage [14] for helium which explicitly contain the r_{12} coordinate. However, the TCDW-IEM ignores the dynamic electron correlations and computes the total probability for the TI as the product of the individual probabilities for transfer of one electron and independent ionization of the other electron [10]. The resulting total cross sections $\sigma_{if}^{\text{TCDW-IEM}}$ are found to largely overestimate the experimental data [6,10]. Singhal and Lin [12] used a coupled-channel semiclassical impact-parameter model with the traveling atomic orbital expansion to calculate the cross sections for single-electron transitions at intermediate impact energies. They combined these probabilities within the IPM applied to collisions of fully stripped projectiles with helium in order to determine cross sections for the TI, DC, and DI. Their theoretical results for the TI in He^{2+}-He are considerably larger than the corresponding experimental data. The total cross sections for the TI have also been calculated by Bhattacharyya *et al.* [21] for the Li^{3+}-He collision above 100 keV/amu within a relativistically covariant field-theoretical approach using the second-order Feynman diagrams. The obtained total cross sections are also much larger than the measured values.

A radically different strategy is provided by using the four-particle scattering theory [15–19]. In this formalism, both static and dynamic electron correlations are automatically included through the perturbation potentials and/or scattering wave functions. An approach along these lines for the DC has recently been devised within the four-body continuum distorted wave (CDW-4B) approximation [15]. When

applied to the DC in fast H^+-He collisions and compared with the experimental data, the CDW-4B was conclusively shown to be superior to the CDW-IPM or TCDW-IEM [15,16]. The same observation was later reported on the DC involving other bare projectiles with the helium target [17] as well as on the RTE and NTE encompassing the $S^{15+}(1s)$-$H(1s)$ scattering [19]. The goal of the present work is to extend the CDW-4B method to ionizing collisions and particularly to the TI.

Atomic units will be used throughout unless stated otherwise.

II. THEORY

Consider a collision in which a bare nucleus P of charge Z_P is impinging upon a heliumlike atomic system consisting of two electrons e_1 and e_2 initially bound to the target nucleus T of charge Z_T. During this collision one electron is captured, while the other is simultaneously ionized, i.e.:

$$Z_P+(Z_T;e_1,e_2)_i\rightarrow(Z_P;e_1)_{f_1}+Z_T+e_2(\vec{\kappa}). \quad (2.1)$$

The parentheses indicate the bound states, the quantum numbers of which are given by the collective labels i or f_1, whereas $\vec{\kappa}$ represents the momentum vector of the ejected electron e_2 with respect to its parent nucleus T. We adopt the quantum-mechanical nonrelativistic spin-independent formalism, which allows one to consider the two electrons as being distinguishable from each other in (2.1). Let $\vec{s}_{1,2}$ and $\vec{x}_{1,2}$ be the position vectors of the electrons $e_{1,2}$ relative to P and T, respectively. Further, let $\vec{R}$ be the position vector of P with respect to T. The corresponding interelectron distance is denoted by $r_{12}=|\vec{s}_1-\vec{s}_2|=|\vec{x}_1-\vec{x}_2|$. The complete Schrödinger equation for the entire system is given by

$$H\Psi=E\Psi, \quad (2.2)$$

where H is the full Hamiltonian,

$$H=H_0+V\equiv V_{P_1}+V_{P_2}+V_{T_1}+V_{T_2}+V_{12}+V_{PT}, \quad (2.3)$$

$$V_{P_j}=-\frac{Z_P}{s_j}, \quad V_{T_j}=-\frac{Z_T}{x_j} \quad (j=1,2), \quad (2.4)$$

$$V_{PT}=\frac{Z_PZ_T}{R}, \quad V_{12}=\frac{1}{r_{12}}. \quad (2.5)$$

The total energy is denoted by E and it can be expressed through its conservation law:

$$E=E_i+\frac{k_i^2}{2\mu_i}=(E_{f_1}+E_\kappa)+\frac{k_f^2}{2\mu_f}, \quad (2.6)$$

$$E_{f_1}=-\frac{Z_P^2}{2n_{f_1}^2}, \quad E_\kappa=\frac{\kappa^2}{2}. \quad (2.7)$$

Here, μ_i and μ_f are the reduced masses in the entrance and exit channel, $\mu_i=m_P(m_T+2)/m$, $\mu_f=m_T(m_P+2)/m$, $m=m_P+m_T+2$, where m_P and m_T are masses of the projectile and the target, respectively. The vectors $\vec{k}_i$ and $\vec{k}_f$ are the initial and final momenta of the scattering aggregates. The observables E_i and $E_{f_1}+E_\kappa$ are the initial and final *exact* electronic energies. In the case of the helium target, the remarkable variational estimate

$$E_i=-2.903\ 724\ 377\ 034\ 105,$$

obtained by Drake [22] via a fully correlated ~600-term Hylleraas wave function with an explicit allowance of the r_{12} coordinate could rightly be considered as being the exact value. Neglect of the mass-polarization terms $-\vec{\nabla}_1\cdot\vec{\nabla}_2/m_P$ and $-\vec{\nabla}_1\cdot\vec{\nabla}_2/m_T$, in accordance with the eikonal limit $m_{P,T}\gg1$, will enable one to write the four-body kinetic energy operator H_0 in the following separable and additive form:

$$\begin{aligned}H_0&=-\frac{1}{2\mu_i}\nabla_{r_i}^2-\frac{1}{2b_1}\nabla_{x_1}^2-\frac{1}{2b_2}\nabla_{x_2}^2\\&\equiv-\frac{1}{2\mu_i}\nabla_{r_i}^2+H_{0T}\\&=-\frac{1}{2\mu_f}\nabla_{r_f}^2-\frac{1}{2a_1}\nabla_{s_1}^2-\frac{1}{2a_2}\nabla_{s_2}^2\\&\equiv-\frac{1}{2\mu_f}\nabla_{r_f}^2+H_{0P}.\end{aligned} \quad (2.8)$$

The vector $\vec{r}_i$ relates the P to the center of mass of the target in the entrance channel, whereas $\vec{r}_f$ is the position vector of T with respect to the center of mass of the system $(Z_P,e_1)_{f_1}+e_2$ in the exit channel. These relative vectors can be connected to the electronic coordinates $\vec{x}_{1,2}$ and $\vec{s}_{1,2}$ via the expressions

$$\begin{aligned}\vec{r}_i&=\frac{b}{2}(\vec{x}_1+\vec{x}_2)-\frac{1}{2}(\vec{s}_1+\vec{s}_2),\\\vec{r}_f&=\frac{a}{2}(\vec{s}_1+\vec{s}_2)-\frac{1}{2}(\vec{x}_1+\vec{x}_2),\end{aligned} \quad (2.9)$$

where $a=m_P/(m_P+2)$, $b=m_T/(m_T+2)$, $a_1=a_2=m_P/(m_P+1)$, and $b_1=b_2=m_T/(m_T+1)$. As usual for rearranging collisions, the complete Hamiltonian H from Eq. (2.3) is further split into the following two equivalent relations:

$$H=H_i+V_i=H_f+V_f. \quad (2.10)$$

Here, $V_{i,f}$ and $H_{i,f}$ are the perturbations and channel Hamiltonians in the initial and final states, respectively:

$$H_i=H_0+V_T, \quad H_f=H_0+V_P, \quad (2.11)$$

$$V_i=V-V_T, \quad V_f=V-V_P, \quad (2.12)$$

$$V_T=V_{T1}+V_{T2}+V_{12}, \quad V_P=V_{P_1}. \quad (2.13)$$

The unperturbed channel states Φ_i and Φ_f are defined by

$$(H_i-E)\Phi_i=0, \quad (H_f-E)\Phi_f=0, \quad (2.14)$$

$$\Phi_i=\varphi_i(\vec{x}_1,\vec{x}_2)e^{i\vec{k}_i\cdot\vec{r}_i}, \quad (2.15)$$

$$\Phi_f=\varphi_{f_1}(\vec{s}_1)\phi_f, \quad \phi_f=(2\pi)^{-3/2}e^{-i\vec{k}_f\cdot\vec{r}_f+i\vec{\kappa}\cdot\vec{x}_2}. \tag{2.16}$$

The object $\varphi_i(\vec{x}_1,\vec{x}_2)$ represents the two-electron bound state wave function of the atomic system $(Z_T;e_1,e_2)_i$, whereas $\varphi_{f_1}(\vec{s}_1)$ is the single-electron hydrogenlike wave function of $(Z_P,e_1)_{f_1}$ in the exit channel. The complete wave function from Eq. (2.2) must obey the correct boundary conditions:

$$\Psi_i^+ \underset{r_i\to\infty}{\to} \Phi_i e^{i\nu_i \ln(k_i r_i-\vec{k}_i\cdot\vec{r}_i)}\equiv\Phi_i^+, \tag{2.17a}$$

$$\Psi_f^- \underset{r_f\to\infty,x_2\to\infty}{\longrightarrow} \Phi_f e^{-i\nu_f \ln(k_f r_f-\vec{k}_f\cdot\vec{r}_f)+i(Z_T/\kappa)\ln(\kappa x_2+\vec{\kappa}\cdot\vec{x}_2)}\equiv\Phi_f^-, \tag{2.17b}$$

where

$$\nu_i=\frac{Z_P(Z_T-2)}{v}, \quad \nu_f=\frac{(Z_P-1)(Z_T-1)}{v}, \tag{2.18}$$

with $\vec{v}$ being the vector of the incident velocity. Thus, the initial Φ_i and final Φ_f states and are distorted in their respective channels even at infinity due to the presence of the asymptotic Coulomb potentials.

In order to describe the double transition (2.1) at high impact energies, we shall start from the following expression for the ''prior'' and ''post'' transition amplitudes [23,24]:

$$T_{if}^-=\langle\Phi_f|\Omega_f^{-\dagger}[1+G_x^+(V_f-W_f)]^\dagger(V_i-W_i)\Omega_i^+|\Phi_i\rangle, \tag{2.19a}$$

$$T_{if}^+=\langle\Phi_f|\Omega_f^{-\dagger}(V_f-W_f)^\dagger[1+G_x^+(V_i-W_i)]\Omega_i^+|\Phi_i\rangle, \tag{2.19b}$$

where Ω_i^+ and Ω_f^- are Møller wave operators,

$$\Omega_{i,f}^\pm=1+G_{i,f}^\pm W_{i,f}, \quad G_{i,f}^\pm=(E-H_{i,f}-W_{i,f}\pm i\epsilon)^{-1}. \tag{2.20}$$

Here, $W_{i,f}$ are certain distorting potentials and ϵ is an infinitesimally small positive number ($\epsilon\to0^+$). The transition amplitudes (2.19a), (2.19b) are free from the so-called disconnected diagrams [25,26]. These Feynman diagrams would correspond to divergent matrix elements for those collisional paths describing two constituents interacting with each other in the presence of a third freely propagating particle. Since the free motion is mediated via the free-particle Green's resolvents $G_0^\pm=1/(E-H_0\pm i\epsilon)$, it is clear that the typical kernels $(V_f-W_f)^\dagger G_0^\pm(V_i-W_i)$ from the *iterated* transition T operator would not contain any disconnected diagrams if no two-body interaction in the perturbation V_f-W_f is repeated in V_i-W_i. This can be achieved through introduction of an intermediate channel propagator G_x^+, such as

$$G_x^+=(E-H+V_x+i\epsilon)^{-1}, \tag{2.21a}$$

possessing a model potential operator V_x, which must be chosen in accordance with the mentioned constraints on the distorting potentials $W_{i,f}$. In the distorted-wave formalism, instead of solving directly the full Schrödinger equation (2.2) with rigidly determined interactions, one customarily considers a model problem possessing certain auxiliary, flexible potentials and defines the distorted waves χ_i^+ and χ_f^- through

$$\chi_i^+=\Omega_i^+\Phi_i, \quad \chi_f^-=\Omega_f^-\Phi_f. \tag{2.21b}$$

In the limit $\epsilon\to0^+$, these scattering states satisfy the equations

$$(E-H_i-W_i)|\chi_i^+\rangle=0, \quad (E-H_f-W_f)|\chi_f^-\rangle=0. \tag{2.21c}$$

The original problem (2.2) is retrieved from the model equation (2.21c) by the physical requirement that the scattering states $\chi_{i,f}^\pm$ must asymptotically coincide with the associated total wave functions $\Psi_{i,f}^\pm$, respectively. The transition amplitude (2.19) can now be rewritten in terms of the distorted waves $\chi_{i,f}^\pm$ as

$$T_{if}^-=\langle\xi_f^-|U_i|\chi_i^+\rangle, \quad T_{if}^+=\langle\chi_f^-|U_f^\dagger|\xi_i^+\rangle, \tag{2.22}$$

where

$$|\xi_{i,f}^\pm\rangle=(1+G_x^\pm U_{i,f})|\chi_{i,f}^+\rangle, \quad U_{i,f}=V_{i,f}-W_{i,f}. \tag{2.23}$$

We shall first determine the distorted wave χ_i^+ in the entrance channel. Imposing the boundary condition: $\chi_i^+\underset{r_i\to\infty}{\to}\Psi_i^+$, we look for χ_i^+ in a factored form, such as

$$\chi_i^+=\varphi_i(\vec{x}_1,\vec{x}_2)\mathcal{G}_i^+. \tag{2.24}$$

Inserting Eq. (2.24) into Eq. (2.21c), we obtain

$$\varphi_i(E-E_i-H_0-V_i)\mathcal{G}_i^+ + \sum_{j=1}^{2}\frac{1}{b_j}\vec{\nabla}_{x_j\varphi_i}\cdot\vec{\nabla}_{s_j}\mathcal{G}_i^+ + U_i\chi_i^+ + \mathcal{G}_i^+(E_i-H_T)\varphi_i=0, \tag{2.25}$$

where H_T is the target Hamiltonian ($H_T=H_{0T}+V_T$). In order to solve Eq. (2.25) without any further approximations, we shall make the following choice for distorting potential U_i:

$$U_i=Z_P\left(\frac{1}{R}-\frac{1}{s_2}\right)-\left[\sum_{j=1}^{2}\frac{1}{b_j}\vec{\nabla}_{x_j}\varphi_i\cdot\vec{\nabla}_{s_j}+O_{\varphi_i}\right]\circ\frac{1}{\varphi_i}, \tag{2.26a}$$

where

$$O_{\varphi_i}\equiv O_{\varphi_i}(\vec{x}_1,\vec{x}_2)=(E_i-H_{T,\varphi_i})\varphi_i(\vec{x}_1,\vec{x}_2). \tag{2.26b}$$

An equivalent expression of (2.26a) is given by $U_i=Z_P(1/R-1/s_2)-(1/b_1)\vec{\nabla}_{x_1}\ln\varphi_i\cdot\vec{\nabla}_{s_1}-(1/b_2)\vec{\nabla}_{x_2}\ln\varphi_i\cdot\vec{\nabla}_{s_2}+O_{\varphi_i}$. The possible nodes of φ_i would render U_i singular. In order to bypass this difficulty, we introduce the symbol $\circ$ in Eq. (2.26a) to indicate that U_i acts only on those functions which contain φ_i in the factored form, as exemplified by Eq. (2.24). Moreover, the Hamiltonian H_T in Eq. (2.26a) operates only on φ_i and this is emphasized in (2.26b) through the notation $H_T\equiv H_{T,\varphi_i}$. Hence,

$$U_i\chi_i^+ = Z_P\left(\frac{1}{R}-\frac{1}{s_2}\right)\chi_i^+ - \sum_{j=1}^{2}\frac{1}{b_j}\vec{\nabla}_{x_j}\varphi_i\cdot\vec{\nabla}_{s_j}\mathcal{G}_i^+ - \mathcal{G}_i^+ O_{\varphi_i}. \tag{2.26c}$$

Using the mass limit $m_{P,T}\gg 1$ together with the resulting simplification $\vec{R}\simeq -\vec{r}_f$, we obtain an equation for $\mathcal{G}_i^+$, such as

$$\left[E-E_i-H_0+\frac{Z_P}{s_1}-\frac{Z_P(Z_T-1)}{r_f}\right]\mathcal{G}_i^+ = 0, \tag{2.27a}$$

which can be solved exactly, yielding

$$\mathcal{G}_i^+ = C_i^+\,\varphi^+_{\vec{p}_1}(\vec{s}_1)\,\phi_{\vec{p}_2}(\vec{s}_2)\,\varphi^+_{\vec{p}_f}(\vec{r}_f), \tag{2.27b}$$

where C_i^+ is a constant and $\phi_{\vec{\omega}}(\vec{r})$ is a plane wave. The Coulomb waves with the outgoing and incoming boundary conditions are respectively labeled by $\varphi^+_{\vec{\omega}}(\vec{r})$ and $\varphi^-_{\vec{\omega}}(\vec{r})$, the explicit expressions of which are

$$\varphi^+_{\vec{p}_1}(\vec{s}_1) = \Gamma(1-i\nu'_P)e^{\pi\nu'_P/2+i\vec{p}_1\cdot\vec{s}_1}{}_1F_1(i\nu'_P,1,ip_1s_1 - i\vec{p}_1\cdot\vec{s}_1), \tag{2.28}$$

$$\phi_{\vec{p}_2}(\vec{s}_2) = e^{i\vec{p}_2\cdot\vec{s}_2}, \tag{2.29}$$

$$\varphi^+_{\vec{p}_f}(\vec{r}_f) = \Gamma(1+i\nu')e^{-\pi\nu'/2+i\vec{p}_f\cdot\vec{r}_f}{}_1F_1(-i\nu',1,ip_fr_f - i\vec{p}_f\cdot\vec{r}_f). \tag{2.30}$$

Here, ${}_1F_1$ denotes the usual Kummer confluent hypergeometric function with the Sommerfeld parameters $\nu'_P = Z_Pa_1/p_1$ and $\nu' = Z_P(Z_T-1)\mu_f/p_f$. The vectors $\vec{p}_1$, $\vec{p}_2$, and $\vec{p}_f$ must satisfy the energy conservation law and preserve the form of the asymptotic plane wave $\exp(i\vec{k}_i\cdot\vec{r}_i)$ in the entrance channel. This indeed will be the case provided that

$$E-E_i = \frac{p_1^2}{2a_1}+\frac{p_2^2}{2a_2}+\frac{p_f^2}{2\mu_f}, \tag{2.31}$$

$$\vec{p}_1\cdot\vec{s}_1+\vec{p}_2\cdot\vec{s}_2+\vec{p}_f\cdot\vec{r}_f = \vec{k}_i\cdot\vec{r}_i. \tag{2.32}$$

Using the relation $\vec{r}_i = -b\vec{r}_f - a(\vec{s}_1+\vec{s}_2)/\mu_i$ and the mass limit $m_{P,T}\gg 1$, it immediately follows from Eq. (2.32) that the auxiliary intermediate momentum vectors $\vec{p}_1$, $\vec{p}_2$, and $\vec{p}_f$ are identified as

$$\vec{p}_1 = \vec{p}_2 = -\frac{a}{\mu_i}\vec{k}_i = -a\vec{v}_i \simeq -\vec{v}, \tag{2.33}$$

$$\vec{p}_f = -b\vec{k}_i \simeq -\vec{k}_i. \tag{2.34}$$

Finally, leaving out the unimportant phase factor $C_i^+ = \mu_i^{-i\nu_P}$, the distorted wave χ_i^+ reduces to

$$\chi_i^+ = N^+(\nu_P)\mathcal{N}^+(\nu)e^{i\vec{k}_i\cdot\vec{r}_i}\varphi_i(\vec{x}_1,\vec{x}_2){}_1F_1(i\nu_P,1,iv s_1 + i\vec{v}\cdot\vec{s}_1)\ {}_1F_1(-i\nu,1,ik_ir_f+i\vec{k}_i\cdot\vec{r}_f), \tag{2.35}$$

$$N^+(\nu_P) = \Gamma(1-i\nu_P)e^{\pi\nu_P/2}, \quad \mathcal{N}^\pm(\nu) = \Gamma(1\pm i\nu)e^{-\pi\nu/2}, \tag{2.36}$$

$$\nu_P = \frac{Z_P}{v}, \quad \nu = \frac{Z_P(Z_T-1)}{v}. \tag{2.37}$$

It is easily verified that the scattering state χ_i^+ exhibits the required eikonal asymptotic behavior: $\chi_i^+ \underset{r_i\to\infty}{\to} \Phi_i^+$. The term O_{φ_i} in Eq. (2.26a) vanishes identically *only* for the *exact* eigensolutions φ_i and E_i of the target Hamiltonian H_T. However, since these are unavailable, the term O_{φ_i} should, in principle, be kept throughout, as originally suggested in Ref. [27] in the four-body corrected first Born (CB1-4B) approximation for the DC.

Next, we shall look for the distorted wave ξ_f^- which satisfies the equation

$$(E-H+V_x-i\epsilon)|\xi_f^-\rangle = -(i\epsilon-V_x)|\chi_f^-\rangle, \tag{2.38a}$$

which is obtained from Eq. (2.23). Choosing the intermediate channel potential V_x in such a way that the constraint,

$$V_x|\chi_f^-\rangle = 0, \tag{2.38b}$$

is automatically satisfied, we shall have, in the limit $\epsilon\to 0^+$:

$$(E-H+V_x)|\xi_f^-\rangle = 0. \tag{2.38c}$$

Writing ξ_f^- in a factored form similar to χ_i^+:

$$\xi_f^- = \varphi_{f_1}\mathcal{G}_f^-, \tag{2.39}$$

we arrive at

$$\mathcal{G}_f^-(E_f-H_0-V_P)\varphi_{f_1} + \varphi_{f_1}(E-E_f-H_0-V_f)\mathcal{G}_f^- + \frac{1}{a_1}\vec{\nabla}_{s_1}\varphi_{f_1}\cdot\vec{\nabla}_{x_1}\mathcal{G}_f^- + V_x\xi_f^- = 0. \tag{2.40}$$

Analogous with Eq. (2.25), we intend to find the solutions of Eq. (2.40) in the pertinent mass limit $m_{P,T}\gg 1$ without any further approximations. This can be accomplished by choosing the model potential V_x, for example, as

$$V_x = Z_P\left(\frac{1}{R}-\frac{1}{s_2}\right)-\left(\frac{1}{x_1}-\frac{1}{r_{12}}\right)-\frac{1}{a_1}\vec{\nabla}_{s_1}\varphi_{f_1}\cdot\vec{\nabla}_{x_1}\circ\frac{1}{\varphi_{f_1}}. \tag{2.41}$$

Hence, in the mentioned heavy mass limit, Eq. (2.41), is reduced to the equation

$$\left[E-E_f-H_0+\frac{Z_T-1}{x_1}+\frac{Z_T}{x_2}-\frac{Z_P(Z_T-1)}{r_i}\right]\mathcal{G}_f^- = 0, \tag{2.42}$$

which can be solved exactly due to separation of the independent variables. Again the meaning of the symbol $\circ$ in Eq. (2.41) determines the domain of definition of the operator V_x, which is allowed to act only onto a subspace of the complete Hilbert space containing wave functions with the factored hydrogenlike bound state φ_{f_1}, as in (2.39). We search for $\mathcal{G}_f^-$ in the separable form:

$$\mathcal{G}_f^- = C_f^-\,\varphi^-_{\vec{q}_1}(\vec{x}_1)\,\varphi^-_{\vec{q}_2}(\vec{x}_2)\,\varphi^-_{\vec{q}_i}(\vec{r}_i), \tag{2.43}$$

with C_f^- being an overall constant, and

$$\varphi^-_{\vec{q}_1}(\vec{x}_1)=\Gamma(1+i\nu'_T)e^{\pi\nu'_T/2+i\vec{q}_1\cdot\vec{x}_1}{}_1F_1(-i\nu'_T,1,-iq_1x_1 - i\vec{q}_1\cdot\vec{x}_1), \tag{2.44}$$

$$\varphi^-_{\vec{q}_2}(\vec{x}_2)=\Gamma(1+i\zeta')e^{\pi\zeta'/2+i\vec{q}_2\cdot\vec{x}_2}{}_1F_1(-i\zeta',1,-iq_2x_2 - i\vec{q}_2\cdot\vec{x}_2), \tag{2.45}$$

$$\varphi^-_{\vec{q}_i}(\vec{r}_i)=\Gamma(1-i\nu'')e^{-\pi\nu''/2+i\vec{q}_i\cdot\vec{r}_i}{}_1F_1(i\nu'',1,-iq_ir_i - i\vec{q}_i\cdot\vec{r}_i), \tag{2.46}$$

where $\nu'_T=(Z_T-1)b_1/q_1$, $\zeta'=Z_Tb_2/q_2$, and $\nu''=Z_P(Z_T-1)\mu_i/q_i$. We impose the conservation of energy in the exit channel via

$$E-E_f=\frac{q_1^2}{2b_1}+\frac{q_2^2}{2b_2}+\frac{q_i^2}{2\mu_i}, \tag{2.47}$$

as well as preservation of the form of the three free-particle plane wave $\exp(-i\vec{k}_f\cdot\vec{r}_f+i\vec{\kappa}\cdot\vec{x}_2)$:

$$\vec{q}_1\cdot\vec{x}_1+\vec{q}_2\cdot\vec{x}_2+\vec{q}_i\cdot\vec{r}_i=-\vec{k}_f\cdot\vec{r}_f+\vec{\kappa}\cdot\vec{x}_2. \tag{2.48}$$

These two conditions, together with the relation: $\vec{r}_f=-a\vec{r}_i-b(\vec{x}_1+\vec{x}_2)/\mu_f$ and the subsequent mass limit $m_{P,T}\gg1$ lead to

$$\vec{q}_1=\frac{a}{\mu_f}\vec{k}_f\simeq\frac{1}{\mu_f}\vec{k}_f\simeq\vec{v},\quad \vec{q}_i=a\vec{k}_f\simeq\vec{k}_f, \tag{2.49a}$$

$$\vec{q}_2=\frac{a}{\mu_f}\vec{k}_f+\vec{\kappa}\simeq\frac{1}{\mu_f}\vec{k}_f+\vec{\kappa}\simeq\vec{p}, \tag{2.49b}$$

where

$$\vec{p}=\vec{v}+\vec{\kappa}. \tag{2.49c}$$

Thus, the distorted wave $\xi_f^-=\varphi_{f_1}\mathcal{G}_f^-$ becomes:

$$\xi_f^-=N^-(\zeta)N^-(\nu_T)\mathcal{N}^-(\nu)\phi_f\varphi_{f_1}(\vec{s}_1)\ {}_1F_1(-i\zeta,1,-ipx_2 - i\vec{p}\cdot\vec{x}_2){}_1F_1(-i\nu_T,1,-iv x_1-i\vec{v}\cdot\vec{x}_1)\ {}_1F_1(i\nu,1, -ik_fr_i-i\vec{k}_f\cdot\vec{r}_i), \tag{2.50}$$

where ϕ_f is defined in Eq. (2.16) and

$$N^-(\zeta)=\Gamma(1+i\zeta)e^{\pi\zeta/2},\quad N^-(\nu_T)=\Gamma(1+i\nu_T)e^{\pi\nu_T/2},$$

$$\zeta=\frac{Z_T}{p},\quad \nu_T=\frac{Z_T-1}{v}. \tag{2.51}$$

It can immediately be checked that the conditions (2.38a) as well as $\chi_f^- \underset{r_f\to\infty}{\to} \Phi_f^-$ are both fulfilled with the present distorted wave χ_f^-. Inserting Eqs. (2.50), (2.35), and (2.26a) into Eq. (2.22) for the ''prior'' transition amplitude, we obtain

$$\begin{aligned}T^-_{if}=N_{PT}\int\int\int d\vec{R}\ d\vec{s}_1d\vec{s}_2e^{i\vec{\alpha}\cdot\vec{s}_1+i\vec{\beta}\cdot\vec{x}_1-i\vec{\kappa}\cdot\vec{x}_2}R_\nu(\vec{r}_i,\vec{r}_f)\varphi^*_{f_1}(\vec{s}_1)\ {}_1F_1(i\nu_T,1,ivx_1+i\vec{v}\cdot\vec{x}_1)\\ \times{}_1F_1(i\zeta,1,ipx_2+i\vec{p}\cdot\vec{x}_2)\left[Z_P\left(\frac{1}{R}-\frac{1}{s_2}\right)\ {}_1F_1(i\nu_P,1,ivs_1+i\vec{v}\cdot\vec{s}_1)\varphi_i(\vec{x}_1,\vec{x}_2)-\vec{\nabla}_{x_1}\varphi_i(\vec{x}_1,\vec{x}_2)\cdot\vec{\nabla}_{s_1}\ {}_1F_1(i\nu_P,1,ivs_1+i\vec{v}\cdot\vec{s}_1)\right.\\ \left.-{}_1F_1(i\nu_P,1,ivs_1+i\vec{v}\cdot\vec{s}_1)O_{\varphi_i}(\vec{x}_1,\vec{x}_2)\right]\\ \equiv T^-_{if;\nu}(\vec{\eta}),\end{aligned} \tag{2.52}$$

where the auxiliary function $O_{\varphi_i}(\vec{x}_1,\vec{x}_2)$ is given by Eq. (2.26b) and

$$R_\nu(\vec{r}_i,\vec{r}_f)=\mathcal{N}^{-*}(\nu)\mathcal{N}^+(\nu)\ {}_1F_1(-i\nu,1,ik_fr_i+i\vec{k}_f\cdot\vec{r}_i) \times{}_1F_1(-i\nu,1,ik_ir_f+i\vec{k}_i\cdot\vec{r}_f), \tag{2.53}$$

$$N_{PT}=(2\pi)^{-3/2}N^+(\nu_P)N^{-*}(\nu_T)N^{-*}(\zeta), \tag{2.54}$$

$$\vec{\alpha}=\vec{\eta}-\left(\frac{v}{2}-\frac{Q}{v}\right)\hat{\vec{v}},\quad \vec{\beta}=-\vec{\eta}-\left(\frac{v}{2}+\frac{Q}{v}\right)\hat{\vec{v}},$$

$$Q=E_i-(E_{f_1}+E_\kappa), \tag{2.55}$$

with $\vec{\eta}$ being the transversal component of the momentum transfer $\vec{k}_i-\vec{k}_f$ with the properties $\vec{\alpha}+\vec{\beta}=-\vec{v}$ and $\vec{\eta}\cdot\vec{v}=0$, where the impact velocity vector $\vec{v}$ is directed along the Z axis. It is because of the underlying charge exchange component of the TI that there are two different momentum transfers in Eq. (2.52), i.e., $\vec{\alpha}=a\vec{k}_f-\vec{k}_i$ and $\vec{\beta}=b\vec{k}_i-\vec{k}_f$, which reduce to Eq. (2.55) in the mass limit $m_{P,T}\gg1$. The relation $\vec{k}_i\cdot\vec{r}_i+\vec{k}_f\cdot\vec{r}_f=\vec{\alpha}\cdot\vec{s}_1+\vec{\beta}\cdot\vec{x}_1$ is also used in Eq. (2.52). The difference $E_i-(E_{f_1}+E_\kappa)$ between the initial and final electronic energies is also known as the inelasticity or Q factor. This observable is of key importance to translational spectroscopy, which through the measurement of the

Q values determines the experimental data on the energy gain or loss of the scattered projectile, i.e., on the inelastic energy transfer.

An analogous derivation is carried out for the ''post'' form of the transition amplitude T_{if}^{+} and we need only to quote the final result as

$$T_{if}^{+}=N_{PT}\int\int\int d\vec{R}\; d\vec{x}_1 d\vec{x}_2 e^{i\vec{\alpha}\cdot\vec{s}_1+i\vec{\beta}\cdot\vec{x}_1-i\vec{\kappa}\cdot\vec{x}_2}R_\nu(\vec{r}_i,\vec{r}_f)\varphi_i(\vec{x}_1,\vec{x}_2)\;{}_1F_1(i\nu_P,1,iv s_1+i\vec{v}\cdot\vec{s}_1){}_1F_1(i\zeta,1,ipx_2+i\vec{p}\cdot\vec{x}_2)$$
$$\times\left\{\left[Z_P\left(\frac{1}{R}-\frac{1}{s_2}\right)+\left(\frac{1}{r_{12}}-\frac{1}{x_1}\right)\right]\;{}_1F_1(i\nu_T,1,ivx_1+i\vec{v}\cdot\vec{x}_1)\varphi_{f_1}^{*}(\vec{s}_1)-\vec{\nabla}_{s_1}\varphi_{f_1}^{*}(\vec{s}_1)\cdot\vec{\nabla}_{x_1}\;{}_1F_1(i\nu_T,1,ivx_1+i\vec{v}\cdot\vec{x}_1)\right\}$$
$$\equiv T_{if;\nu}^{+}(\vec{\eta}). \tag{2.56}$$

A considerable simplification in calculation can be obtained by employing the following approximation:

$$R_\nu(\vec{r}_i,\vec{r}_f)\underset{\mu\to\infty}{\simeq}(\mu\rho v)^{2i\nu}, \tag{2.57}$$

which can be easily derived in the indicated mass limit. Here, μ is the reduced mass of P and T, i.e., $\mu=m_P m_T/(m_P+m_T)$, whereas the projection of the vector $\vec{R}$ onto the $\vec{v}$ axis is denoted by $\vec{\rho}$, which need not necessarily be identified with the usual impact parameter of the IPM. It is easy to see that the phase factor $(\mu\rho v)^{2i\nu}=(\mu\rho v)^{2iZ_P(Z_T-1)/v}$ does not contribute to the total cross sections $\sigma_{if}^{\pm}$. A part of this phase, namely, the term $(\mu\rho v)^{2iZ_PZ_T/v}$, incorporates the entire contribution to the $T_{if}^{\pm}$ from the potential $V_{PT}=Z_PZ_T/R$. Hence, the internuclear repulsion V_{PT}, which we accounted for *exactly* in the mass limit $m_{P,T}\gg 1$ and the accompanying small values of ϑ_P (the eikonal approximation), does not contribute at all to $\sigma_{if}^{\pm}$. The triple differential cross sections for (2.1) take the following forms:

$$\sigma_{if}^{\pm}(\vec{\kappa})\equiv\frac{d^3\sigma_{if}^{\pm}}{d\vec{\kappa}}=\int d\vec{\eta}\left|\frac{T_{if;\nu}^{\pm}(\vec{\eta})}{2\pi v}\right|^2=\int d\vec{\eta}\left|\frac{T_{if;0}^{\pm}(\vec{\eta})}{2\pi v}\right|^2$$
$$=\int d\vec{\eta}\,|\mathcal{T}_{if}(\vec{\eta})|^2, \tag{2.58a}$$

where

$$\mathcal{T}_{if}^{\pm}(\vec{\eta})=\frac{T_{if;0}^{\pm}(\vec{\eta})}{2\pi v}. \tag{2.58b}$$

Finally, the total cross section for the process (2.1) is given by

$$\sigma_{if}^{\pm}=\int d\vec{\kappa}\;\sigma_{if}^{\pm}(\vec{\kappa}). \tag{2.59}$$

The final expressions (2.52) and (2.56) for the $T_{if}^{\pm}$ constitute the present four-body continuum distorted wave (CDW-4B) approximation for the general TI process (2.1). Although the same type of approximation has been invoked in the prior T_{if}^{-} and the post T_{if}^{+} forms, the obtained expressions (2.52) and (2.56) are very different from each other due to the unequal perturbation potentials $U_i\neq U_f$, where

$$U_i=Z_P\left(\frac{1}{R}-\frac{1}{s_2}\right)$$
$$-\left[\sum_{j=1}^{2}\frac{1}{b_j}\vec{\nabla}_{x_j}\varphi_i\cdot\vec{\nabla}_{s_j}+(E_i-H_{T,\varphi_i})\varphi_i\right]\circ\frac{1}{\varphi_i}, \tag{2.61}$$

and

$$U_f=Z_P\left(\frac{1}{R}-\frac{1}{s_2}\right)-\left(\frac{1}{x_1}-\frac{1}{r_{12}}\right)-\frac{1}{a_1}\vec{\nabla}_{s_1}\varphi_{f_1}\cdot\vec{\nabla}_{x_1}\circ\frac{1}{\varphi_{f_1}}. \tag{2.62}$$

Both U_i and U_f describe the standard Thomas P-e-T double scattering: (i) In the prior form (2.52) for T_{if}^{-}, this is accomplished through the portion of U_i comprised of the symmetrized potential operators $\mathcal{M}_i(\vec{x}_1,\vec{x}_2;\vec{s}_1,\vec{s}_2)=\mathcal{M}_{i_1}(\vec{x}_1,\vec{s}_1)+\mathcal{M}_{i_2}(\vec{x}_2,\vec{s}_2)$, which are concerned with the two independent Thomas double scatterings P-e_1-T and P-e_2-T, where

$$\mathcal{M}_{i_1}(\vec{x}_1,\vec{s}_1)=\vec{\nabla}_{x_1}\ln\varphi_i(\vec{x}_1,\vec{x}_2)\cdot\vec{\nabla}_{s_1},$$
$$\mathcal{M}_{i_2}(\vec{x}_2,\vec{s}_2)=\vec{\nabla}_{x_2}\ln\varphi_i(\vec{x}_1,\vec{x}_2)\cdot\vec{\nabla}_{s_2}. \tag{2.63}$$

However, due to the present simplification manifested via the absence of any function $f(\vec{s}_2)$ in the scattering states $\chi_{i,f}^{\pm}$ of the proposed CDW-4B model, the operator $\mathcal{M}_i(\vec{x}_1,\vec{x}_2;\vec{s}_1,\vec{s}_2)$ reduces merely to $\mathcal{M}_{i_1}(\vec{x}_1,\vec{s}_1)$ associated with P-e_1-T. (ii) In the post form (2.56) of T_{if}^{+}, the classical Thomas P-e_1-T mechanism is described by the following part of the perturbation U_f:

$$\mathcal{M}_{f_1}(\vec{s}_1,\vec{x}_1)=-\vec{\nabla}_{s_1}\ln\varphi_{f_1}(\vec{s}_1)\cdot\vec{\nabla}_{x_1}. \tag{2.64}$$

The single-particle operators $\mathcal{M}_{i_1}(\vec{x}_1,\vec{s}_1)$ and $\mathcal{M}_{f_1}(\vec{s}_1,\vec{x}_1)$ are capable of providing the corresponding quantum-mechanical counterpart of the Thomas P-e_1-T double scattering due to the fact that they depend upon the set of the coordinates $\{\vec{x}_1,\vec{s}_1\}$ which *couple together* the two Coulomb centers $\{Z_P,Z_T\}$ and, hence, mediate the transfer of the electron e_1 from the target T to the projectile P. Both objects $\mathcal{M}_{i_1}(\vec{x}_1,\vec{s}_1)$ and $\mathcal{M}_{f_1}(\vec{s}_1,\vec{x}_1)$ are otherwise reminiscent of the full transition T operator of the three-body continuum

distorted wave (CDW-3B) approximation for a pure hydrogenlike charge exchange [23,24]:

$$Z_P+(Z_T,e)_i\rightarrow(Z_P,e)_f+Z_T, \tag{2.65}$$

with $e=e_1$, $\{i,f\}=\{i_1,f_1\}$, and $\vec{x}=\vec{x}_1$, $\vec{s}=\vec{s}_1$. The operators $\mathcal{M}_i(\vec{x}_1,\vec{x}_2;\vec{s}_1,\vec{s}_2)$ and $\mathcal{M}_{f_1}(\vec{x}_1,s_1)$ from U_i and U_f emerge from the application of the Laplacians $-\nabla^2_{x_1}/(2b_1)$ $-\nabla^2_{x_2}/(2b_2)$ and $-\nabla^2_{s_1}/(2a_1)-\nabla^2_{s_2}/(2a_2)$ onto $\chi^{\pm}_{i,f}$, which are of the separable forms $\varphi_i(\vec{x}_1,\vec{x}_2)\varphi^{+}_{-\vec{k}_i}(\vec{r}_f)\varphi^{+}_{-\vec{v}}(\vec{s}_1)$ and $\varphi_{f_1}(\vec{s}_1)\varphi^{-}_{-\vec{k}_f}(\vec{r}_i)\varphi^{-}_{\vec{v}}(\vec{x}_1)\varphi^{-}_{\vec{p}}(\vec{x}_2)$. Moreover, with a suitable change of the independent variables in H_0, the electron-mass polarizations $\mathcal{M}_{i_1}(\vec{x}_1,\vec{s}_1)$ and $\mathcal{M}_{i_2}(\vec{x}_2,\vec{s}_2)$ would appear as the *perturbation* potential operators along with the more conventional Coulomb interactions $Z_PZ_T/R-Z_P/s_1-Z_P/s_2$ in V_i. However, in contrast to, e.g., the *single-center* local interactions $V_{PT}(R)=Z_PZ_T/R$, $V_{P_1}(s_1)=-Z_P/s_1$ and $V_{P_2}(s_2)=-Z_P/s_2$, the electron-mass polarizations $\mathcal{M}_{i_1}(\vec{x}_1,\vec{s}_1)$, $\mathcal{M}_{i_2}(\vec{x}_2,\vec{s}_2)$ and $\mathcal{M}_{f_1}(\vec{s}_1,\vec{x}_1)$ are *two-center* nonlocal distorting pseudopotentials depending upon two coordinates $\vec{x}_j$ and $\vec{s}_j$ of the given electron e_j $(j=1,2)$. Nonlocal pseudopotentials in the form of differential and/or integral operators, which might also be velocity dependent, are customarily encountered in various branches of physics, e.g., the Hartree-Fock model, radiative corrections, meson field theory, etc. [28]. It is now easy to show [29] that $\mathcal{M}_{i_j}(\vec{x}_j,\vec{s}_j)$ exhibits a long-range Coulombic tail in the CDW-4B method and, hence, the question arises whether this potential could be considered as a perturbation *causing* the transition in Eq. (2.1). In traditional collision theory, an interaction is conceived of as being able to produce scattering only if it vanishes asymptotically at infinitely large values of the interparticle separation. This statement is the basis of the concept known as ''asymptotic freedom'' according to which the full scattering states $\Psi^{\pm}_{i,f}$ must reduce to the free wave packets at infinitely large times $t\rightarrow\mp\infty$. This is fully compatible with the indispensable experimental requirement, which demands that in both the remote past and distant future $(t\rightarrow\mp\infty)$, the examined system must remain unperturbed. In other words, at these two extreme times, the system moves *only* under the influence of the channel Hamiltonians $H_{i,f}$. It is only in this way that, for these asymptotic times, we can be sure of having prepared the *free* wave packets $\Phi_{i,f}$ which in the meantime evolve under the action of the channel perturbations $V_{i,f}=H-H_{i,f}$. With this definition of the asymptotically free states one could certainly consider the situations ''before'' $(t\rightarrow-\infty)$ and ''after'' $(t\rightarrow+\infty)$ collision as being separated from each other. Such a circumstance would guarantee that a transition from the initial to the final state of the system occurs solely under the influence of the interaction potential V_i or V_f. If that were not the case, one could not talk at all about the *free* wave packets as $t\rightarrow\mp\infty$. This means that neither the initial or the final state of the system could be prepared (in the sense of being controlled), in which case the very definition of a scattering phenomenon would cease to have any meaning. In such a circumstance, the particles in the incident beam would interact strongly with each other (before even reaching the target) through, e.g., *intrabeam* scatterings or otherwise, and one would not be able to identify the actual perturber of the colliding projectile-target system. However, this convincing and plausible concept is not directly applicable to the Coulomb scattering. Namely, for long-range Coulombic interactions, the asymptotic form of the wave packet is given by the functions $\Phi^{\pm}_{i,f}$, which are different from $\Phi_{i,f}$, as indicated in Eqs. (2.17a) and (2.17b). In such a case, we speak about a departure from the notion of the asymptotic freedom in the above conventional quantum-mechanical sense. The Coulomb interactions always distort the unperturbed channel scattering state through appearance of a logarithmic phase factor, even in the asymptotic scattering region. In the limit of infinite times, corresponding to infinitely large interparticle distances, this phase would yield the logarithmically divergent Møller wave operators $\Omega^{\pm}_{i,f}$, which, in turn, would preclude any mathematically sound definition of the central object of the theory, namely, the scattering S matrix. However, Dollard [30] was able to show that any Coulombic potentials can indeed *make scattering occur*, provided that $\Omega^{\pm}_{i,f}$ are replaced by the Coulomb-Møller wave operators $\Omega^{C(\pm)}_{i,f}$, which contain an extra term canceling automatically the logarithmically divergent phase factor. The resulting regularized nonsingular kernel $\Omega^{C(\pm)}_{i,f}$ would lead to solely connected Feynman diagrams. Moreover, this very same goal can also be achieved by retaining the simpler and much more tractable operators $\Omega^{\pm}_{i,f}$ and choosing the distorting potentials $W_{i,f}$ in such a way that the resulting model scattering states $\chi^{\pm}_{i,f}$ properly incorporate the overall Coulomb logarithmic phase factors due to any Coulombic remainders from the perturbations $V_{i,f}-W_{i,f}$. This has consistently been done in the CDW-3B [23,24] for single capture (SC) and in the CDW-4B for DC [15], RTE, NTE [19] as well as in the TI process (2.1) of the present work.

In the preceeding derivation, the ionizing path for the electron e_2 is described by the Coulomb wave $\varphi^{-}_{\vec{\kappa}}(\vec{x}_2)$ $\equiv N^{-}(\zeta)\phi_{\vec{\kappa}}(\vec{x}_2)\ {}_1F_1(-i\zeta,1,-ipx_2-i\vec{p}\cdot\vec{x}_2)$, with $\phi_{\vec{\kappa}}(\vec{x}_2)$ $=(2\pi)^{-3/2}e^{i\vec{\kappa}\cdot\vec{x}_2}$, $\zeta=Z_T/p$ and $\vec{p}=\vec{\kappa}+\vec{v}$. Even though the appropriate starting *ansatz* in the undistorted scattering state Φ_f is given by the plane wave $\phi_{\vec{\kappa}}(\vec{x}_2)$ centered on T, the present four-body analysis establishes a distortion of $\phi_{\vec{\kappa}}(\vec{x}_2)$ by $N^{-}(\zeta)\ {}_1F_1(-i\zeta,1,-ipx_2-i\vec{p}\cdot\vec{x}_2)$ as a function of the *translated* electron momentum $\vec{\kappa}+\vec{v}\equiv\vec{p}$ and not merely of $\vec{\kappa}$, which one would expect in the plane wave first Born approximation. In addition to $\mathcal{M}_{i_1}(\vec{x}_1,\vec{s}_1)$ and $\mathcal{M}_{f_1}(\vec{s}_1,\vec{x}_1)$ from the prior and post forms, there is a common perturbation:

$$V_P(R,s_2)=Z_P\left(\frac{1}{R}-\frac{1}{s_2}\right), \tag{2.66}$$

in both T^{-}_{if} and T^{+}_{if}. When considered outside the T matrix, the potential $V_{P_2}=-Z_P/s_2$ represents the direct Coulomb interaction between e_2 and Z_P. Its asymptotic value $V^{\infty}_{P_2}(R)$ at large distances s_2 is given by $-Z_P/R$, since $s_2\rightarrow R$ as $R\rightarrow\infty$. Hence, the term $V_P(R,s_2)$ is precisely the difference between the finite and asymptotic value of the same overall *short-range* potential $V_P(R,s_2)=V_{P_2}(s_2)$ $-V^{\infty}_{P_2}(R)$, in accordance with the correct boundary condi-

tion. However, when placed in the T matrices (2.52) or (2.56), the potential V_{P_2} plays the role of a perturbation which *causes* the capture of the electron e_1. This could only occur through some kind of the underlying correlations between e_2 and e_1. For example, a part of the energy received by the electron e_2 in its collision with Z_P could be sufficient to accomplish the transfer of e_1 to the projectile, provided that the e_1-e_2 correlation is active. This is possible as illustrated by the following argument. Using the relation $\vec{R}=\vec{x}_1-\vec{s}_1=\vec{x}_2-\vec{s}_2$, we can write: $|V_P(s_2)/Z_P|=1/s_2=1/|\vec{r}_{12}-\vec{s}_1|$, where $r_{12}=|\vec{r}_{12}|$ is the interelectronic coordinate $\vec{r}_{12}=\vec{x}_1-\vec{x}_2=\vec{s}_1-\vec{s}_2$. The electron e_1 is captured by P in the final bound state $\varphi_{f_1}(\vec{s}_1)$ in the reaction (2.1) and, therefore, s_1 is of the order of Bohr radius a_0. For such small values of s_1, we can develop $1/|\vec{r}_{12}-\vec{s}_1|$ in a power series around $\vec{s}_1$ according to

$$\frac{1}{s_2}=\frac{1}{|\vec{r}_{12}-\vec{s}_1|}=\frac{1}{r_{12}}-\frac{\vec{r}_{12}\cdot\vec{s}_1}{r_{12}^3}+\cdots . \tag{2.67}$$

The second term of the right-hand side of this equation is known as the long-range dipole approximation. From here we can see that the potential $|V_{P_2}(s_2)/Z_P|=1/r_{12}-(\vec{r}_{12}\cdot\vec{s}_1)/r_{12}^3+\cdots$ contains information on the dielectronic correlation e_1-e_2 through the potential $1/r_{12}$. This means that the sole potential $V_{P_2}(s_2)$ between Z_P and e_2 in the $T_{if}^{\pm}$ can indeed lead to capture of the electron e_1, because of the underlying dielectronic correlation, which is inherently present in the e_2's coordinate $\vec{s}_2$ through $\vec{r}_{12}$ since $\vec{s}_2=\vec{s}_1-\vec{r}_{12}$. A relative role of the potential (2.66) can be estimated as follows. Total cross sections are mainly determined by small values of κ. This correspond to a situation where the electron e_2 resides in a close vicinity of the target nucleus. In such a case, x_2 is small and the difference between s_2 and R is negligible, so that the contribution of $V_P(R,s_2)$ to the total cross sections should be modest. An illustration carried out in the next section for He^{2+}-He transfer ionization at 30–1000 keV/amu shows that the relative contribution of the perturbation $V_P(R,s_2)$ varies from 24% at lower to 16% at higher energies. Hence, at sufficiently large impact energies the potential $-1/s_2$ appears to be nearly cancelled by $1/R$.

The post form T_{if}^{+} contains an additional term:

$$V(r_{12},x_1)=\frac{1}{r_{12}}-\frac{1}{x_1}, \tag{2.68}$$

which is completely absent from the T_{if}^{-}. Here the dielectronic interaction $1/r_{12}$ appears explicitly and combined with the initial and final distortion functions on both centers Z_P and Z_T describes the Thomas P-e-e scattering. Hence, when comparing with the experimental data of Mergel *et al.* [31], the post form T_{if}^{+} from Eq. (2.56) should be used throughout. Due to the perturbation $V(r_{12},x_1)$, even the total cross section in the post form should be more adequate than its prior counterpart. Here, it is instructive to draw a parallel between the TI and the corresponding pure single capture of the type:

$$Z_P+(Z_T;e_1,e_2)_i\rightarrow(Z_P,e_1)_{f_1}+(Z_T,e_2)_{f_2}. \tag{2.69}$$

In all the previous applications of the CDW approximation to this process, the simplification $V_P(R,s_2)\approx 0$ has always been made. This amounts for replacement of the potential $1/R$ by $1/s_2$. As in the TI, this could also be roughly justified for the pure SC in Eq. (2.69) at sufficiently high energies for transfer of e_1 without ionization of e_2. The basis for such a justification is the small value of the x_2 coordinate, since the passive electron e_2 in Eq. (2.69) remains *bound* in the target rest $(Z_T,e_2)_{f_2}$. Therefore, $1/s_2-1/R=1/s_2-1/|\vec{s}_2-\vec{x}_2|=1/s_2-(1/s_2+\vec{x}_2\cdot\vec{s}_2/s_2^3+\cdots)=-\vec{x}_2\cdot\vec{s}_2/s_2^3+\cdots$, which should yield small values of $V_P(R,s_2)$ for the SC reaction (2.69), in a fashion similar to the TI in Eq. (2.1). Our recent applications of the CDW-4B method to Eq. (2.69) for $Z_P=Z_T=2$ confirm that the total cross sections computed with and without $V_P(R,s_2)$ in the transition T operator differ from each other by at most 15% at 30–1000 keV/amu.

It is clear from the above analysis that the extent of inclusion of the static and dynamic electron correlations (SEC and DEC, respectively) is governed by the choice of the distorting potentials. The channel Hamiltonians $H_{i,f}$ are defined strictly for two noninteracting aggregates. Therefore, they are capable of including all the SEC, which provides information on quantum-mechanical states $\varphi_{i,f}$ of the scattering partners *before* or *after* the collision. These customary stationary states $\varphi_{i,f}(\vec{r}_1,\vec{r}_2)$ are of primary importance to spectroscopy. However, they also provide the basic input to the asymptotic *scattering* states $\Phi_{i,f}^{\pm}$ built in the remote past as well as in the distant future $(t\rightarrow\mp\infty)$ as the product of $\varphi_{i,f}$ and the wave functions of the relative motion of the two aggregates (for example, in the DC both φ_i and φ_f describe the heliumlike bound states). This would correspond, e.g., in the entrance channel, to an experimental preparation of the target as well as of the incident beam in their respective well-defined states (energy, polarization, spin, etc.) *prior* to scattering when the projectile beam is turned off. In contrast to the SEC, which is unrelated to the very act of collision, the DEC originates entirely from the scattering event. A collision takes place if both the relative velocity v of the two aggregates and their perturbation interaction have nonzero values. The perturbation potential operators $V_{i,f}$ are naturally conceived of as the difference between the total (H) and channel Hamiltonians $H_{i,f}$, i.e., $V_{i,f}=H-H_{i,f}$, and they could directly contain the electronic interaction V_{12}. It is in this manner that the DEC comes into play and appears explicitly in the transition T *operator* as well as in the full scattering states $\Psi_{i,f}^{\pm}$.

The first measurement aimed to detect the DEC in the TI process was carried out by Horsdal *et al.* [7] on the angular distribution of scattered projectiles in the collision $H^+ + He \rightarrow H + He^{2+} + e$ at four impact energies 200, 300, 400, and 500 keV. More specifically, they intended to determine whether there could be any experimental evidence of the Thomas P-e-e scattering [32,33]. This effect is expected to manifest itself through a peak in the angular distribution of scattered projectiles at the critical angle $\vartheta_P^{\text{Thomas}}=0.55$ mrad in the laboratory system of reference. Horsdal *et al.* [7] measured the angle-dependent probabilities for production of He^{2+} in the mentioned TI process and observed a strong enhancement around $\vartheta\approx 0.5\equiv\vartheta_P^{\text{Horsdal}}$. This enhancement of the recorded relative yield (say, Γ) for capture of one elec-

tron *with* and *without* ionization of the other electron occurred at $\vartheta_P^{\text{Horsdal}}$ which is close to $\vartheta_P^{\text{Thomas}}$, and this led Horsdal *et al.* [7] to consider their data as the first evidence of the dynamic electron-electron correlation in the TI. However, this turned out to be false, since it so happened that the same signature at $\vartheta_P^{\text{Horsdal}}$ could also be reproduced within the CDW-IPM [34], which excludes the dynamic e-e correlations altogether from the onset. The enhancement at $\vartheta_P^{\text{Horsdal}}$ obtained in the CDW-IPM is due to a phase interference of the impact parameter transition probability amplitudes for independent electron transfer $\mathcal{A}_{if}^{\pm(T)}(\vec{\rho})$ and ionization $\mathcal{A}_{if}^{\pm(I)}(\vec{\kappa},\vec{\rho})$. The quantities $\mathcal{A}_{if}^{\pm(T)}(\vec{\rho})$ and $\mathcal{A}_{if}^{\pm(I)}(\vec{\kappa},\vec{\rho})$ are obtained by applying the Fourier transforms to the corresponding quantum-mechanical *three-body* T matrices $\mathcal{T}_{if;0}^{\pm(T)}(\eta)$ and $\mathcal{T}_{if;0}^{\pm(I)}(\vec{\kappa},\vec{\eta})$, which are available from, e.g., Ref. [24]. Analogous with the IPM *probability* $\mathcal{P}_{if}^{\pm(TI)}(\vec{\kappa},\rho)=\mathcal{P}_{if}^{\pm(T)}(\rho)\mathcal{P}_{if}^{\pm(I)}(\vec{\kappa},\rho)$, the full ρ-dependent *probability amplitude* $\mathcal{A}_{if}^{\pm(TI)}(\vec{\kappa},\vec{\rho})$ for the composed TI process is given by the product $\mathcal{A}_{if}^{\pm(T)}(\vec{\rho})\mathcal{A}_{if}^{\pm(I)}(\vec{\kappa},\vec{\rho})$. However, the differential cross section $d^5\sigma/d\vec{\kappa}\,d\Omega_P$, as a Hankel transform, requires an integration of $\mathcal{A}_{if}^{\pm(T)}(\vec{\rho})\mathcal{A}_{if}^{\pm(I)}(\vec{\kappa},\vec{\rho})$ over all $\rho\in[0,\infty]$ weighted with the Bessel function $J_{m_{if}}(\eta\rho)$ and the full internuclear contribution $\rho^{2iZ_PZ_T/v}$:

$$\begin{aligned}\frac{d^5\sigma_{if}^{\pm(TI)}}{d\vec{\kappa}\,d\Omega_P}(a_0^2sr^{-1}) &= \left| i\mu v\int_0^\infty d\rho\ \rho^{1+iZ_PZ_T/v} \right. \\ &\quad \left. \times\mathcal{A}_{if}^{\pm(TI)}(\vec{\kappa},\rho)J_{m_{if}}(\eta\rho)\right|^2 \\ &= \left| i\mu v\int_0^\infty d\rho\ \rho^{1+iZ_PZ_T/v}\mathcal{A}_{if}^{\pm(T)}(\rho) \right. \\ &\quad \left. \times\mathcal{A}_{if}^{\pm(I)}(\vec{\kappa},\rho)J_{m_{if}}(\eta\rho)\right|^2, \qquad (2.70)\end{aligned}$$

where $m_{if}=m_f-m_i$ and $m_{i,f}$ are the usual magnetic quantum numbers of the initial and final bound states, respectively. Since in the CDW-IPM, both $\mathcal{A}_{if}^{\pm(T)}(\rho)$ and $\mathcal{A}_{if}^{\pm(I)}\times(\vec{\kappa},\rho)$ are complex numbers, their phases can combine and produce an interference pattern. Such a coherent interference yields an enhancement in Γ and this occurs at nearly the same scattering angle (say $\vartheta^{\text{CDW-IPM}}$) as the value $\vartheta_P^{\text{Horsdal}}$ from Ref. [7]. Thus, Horsdal *et al.* [7] did not provide an evidence of the Thomas P-e-e double scattering, since the same structure in the angular distribution could also be obtained in the IPM without any recourse to the dynamic interelectron correlation. A phase of any wave function has no physical meaning. However, a phase difference of two wave functions can be measured experimentally and, therefore, could represent a physical observable. Hence, a coherent interference of phase factors in Eq. (2.70) for the CDW-IPM might lead to a physical effect. In Eq. (2.70), one does not encounter directly phases of wave functions (since the spatial integrations are already carried out), but various phase factors of the ρ-dependent transition probability amplitudes with a final cummulative effect, which leads to the mentioned enhancement in Γ at $\vartheta^{\text{CDW-IPM}}$. The relation $\vartheta^{\text{CDW-IPM}}\approx\vartheta_P^{\text{Horsdal}}$ appears to be fortuitous. Nevertheless, the clear independent-particle mechanism behind $\vartheta^{\text{CDW-IPM}}$ serves as a counterexample to the conjuctered Thomas P-e-e correlated scattering as the sole reason for enhancement in Γ at $\vartheta_P^{\text{Horsdal}}$. As a consequence of this couterargument provided by the CDW-IPM [34], the measurement of Horsdal *et al.* [7] needs to be reinterpreted. Subsequent work on the angular and/or energy distributions of ejected electrons within TI has been undertaken by Pálinkás *et al.* [8]. In contrast to Ref. [7], which dealt with the singly differential cross sections, Ref. [8] was concerned with the cross section $d^2\sigma/dE_e d\vartheta_e$, which is differential in two observables, the energy E_e and angle ϑ_e of the ejected electron. This double differential cross section is integrated over the scattering angles ϑ_P of the projectile. Concentrating on the cusp condition of equal velocities ($v_i\approx v_e$) of the projectile and the ionized electron in the collision $H^+ + He \rightarrow H + He^{2+} + e$, they searched for yet another signature of the Thomas P-e-e double collision, namely, a maximum in $d^2\sigma/dE_e d\vartheta_e$ at $\vartheta_e=90°$. This Thomas P-e-e peak was indeed experimentally confirmed in a conclusive way at the energy $E_P=1$ MeV of the incident proton corresponding to $E_e=600$ eV of the ejected electron [8]. Pálinkás *et al.* [8] also recorded another maximum in $d^2\sigma/dE_e d\vartheta_e$ at $\vartheta_e=58°$. The mechanism behind this structure is the interaction of the projectile P with each of the target electrons leading to simultaneous single capture and ionization, which is predicted theoretically to occur at $\vartheta_e=60°$. Here, independent ionization is followed by the so-called kinematic capture, based upon the velocity matching mechanism $\vec{v}_e\approx\vec{v}_P$.

The above discussed different pathways within the TI, fall into a larger category of general interactive dynamics of ions and atoms. Understanding the mechanisms behind the ion-atom collisions is absolutely essential for achieving progress in predicting the evolution of quantum scattering systems. Until essentially ten years ago, most of atomic collision experiments were technologically limited to measurements of only a few observables. Due to a paucity of experimental data on the majority of the subtle and detailed features of collision phenomena, the adequacy and reliability of theoretical models could rarely be thoroughly tested. However, recent technological advances have made the goal of the so-called complete experiment practically a reality. A substantial breakthrough has recently been achieved in determination of a complete momentum kinematics of colliding particles with unprecedented precision through the recoil ion momentum spectroscopy (RIMS) [35,36]. The novel variant COLTRIMS (cold target recoil ion momentum spectroscopy) of this powerful and versatile technique is based upon a precooled supersonic gas jet target [36]. Heavy projectiles mainly scatter forward and, therefore, it is very difficult to experimentally determine angular distributions at very high energies where the most intriguing Thomas multiple scatterings take place. The RIMS and COLTRIMS exploit an alternative idea of bypassing the direct measurements of the scattered projectile parameters through recording all the components of the recoil momentum of the target rest, as well as of the ejected electrons for ionizing collisions. The backtransformation via the energy and momentum conservations enables one to retrieve the differential cross sections for the scattered projectiles. The impressive power of this method lies in the fact that its nearly 4π detector efficiency

successfully combines with a very high momentum (Δp) and energy transfer (ΔQ) resolutions irrespective of the impact energy value and, at the same time, exhibits only a very weak dependence upon the energy spread, as well as divergence of the beam. This is in sharp contrast with the customary translational spectroscopy (TS) measuring the energy loss of the projectile, where any gain in the detector efficiency is automatically compromised with loss in energy resolution. The TS measures a change in the impact energy E_P and, hence, relies heavily upon the quality of the projectile beam, its divergence and the energy spread. Implementing, e.g., the COLTRIMS within storage rings, with the electron or laser cooling of both the incoming beam and the target, would be of primary importance in yielding the additional experimental data on higher-order *interelectron* Thomas scatterings. This could provide the most stringent test of atomic collision theory at larger energies beyond the reach of the corresponding single-pass experiments [36]. The COLTRIMS is, in fact, currently being built at the Stockholm storage ring CRYRING, where a reduction by another order of magnitude in $\Delta\vartheta_P$ and ΔQ is anticipated to be within reach at the end of 1996. The success of the COLTRIMS depends critically upon the possibility of high momentum resolution Δp of the recoiled target ion to within a fraction of the atomic unit. At room temperature, such precision is impossible, since the required Δp would lie in the regime of the thermal motion of the target constituents. The difficulty is overcome by cooling the target, so that at the currently reached temperature $\sim$0.1 K, the achieved momentum (in all three directions) and energy resolutions are $\Delta p \approx \pm 0.025$ a.u. and $\Delta Q \approx \pm 6$ eV. Such accuracy in the, e.g., transversal momentum component of the recoiled ion leads to the resolution $\Delta\vartheta_P \approx \pm 1$ μrad in the scattering angle ϑ_P at, e.g., 1 MeV in H^+-He one-electron transfer [36]. This represents a remarkable achievement in comparison to $\Delta\vartheta_P \sim 30$ μrad and $\Delta Q \approx \pm 50$ eV reached by the conventional TS [37]. Such an angular resolution of COLTRIMS provides a unique opportunity to unfold the hidden structures in the differential cross sections at high energies allowing access to various Thomas multiple scatterings. For example, an inspection of the existing experimental data on H^+-H and H^+-He single charge exchange reveals that the width of the Thomas peaks is larger for helium than for an atomic hydrogen target [38,39]. We have shown [40] that such a phenomenon is due to an additional peak originating from the Thomas P-e-e scattering. This structure at $\vartheta_P^{P\text{-}e\text{-}e}$ is very close to the critical angle $\vartheta_P^{PeT} = 0.47$ mrad of the standard Thomas P-e-T double collision. Since the position of $\vartheta_P^{P\text{-}e\text{-}e}$ was not resolved in the previous experiments [38,39], the P-e-e mechanism revealed itself indirectly through widening the observed P-e-T peak. Both Thomas collisions P-e-e and P-e-T are of an intrinsically correlated nature. The former manifests the pure dielectronic correlation, whereas in the latter scattering, the target nucleus is the object of correlation. This belongs to a class of a generalized correlation concept involving only *one electron* and the other arbitrary center of force, which is the target nucleus T in the H^+-He single charge exchange. Obviously, highly correlated events in atomic collisions need not necessarily encompass two electrons. The above-mentioned improvements in $\Delta\vartheta_P$ at the combined COLTRIMS-CRYRING facility could allow one to separate the two pathways P-e-e and P-e-T from each other in an attempt to assess the relative role of these competitive mechanisms behind charge exchange in the high-energy regime $\sim$5–10 MeV/amu. Recently, Mergel *et al.* [31], used the COLTRIMS for the TI in H^+-He and confirmed the results of Ref. [8]. Their goal, however, was to assess the relative role of the mentioned binary kinematic capture accompanied with independent ionization *and* the correlated P-e-e mechanism. They found experimental evidence at $E \geqslant 1$ MeV that the Thomas P-e-e scattering could well dominate the independent event of the kinematic capture and ionization. It is pertinent to recall here, that dominance of e_P-e_T interaction over the P-e_T or T-e_P potentials (the so-called antiscreening effect) has previously been experimentally detected in, e.g., collisions between two hydrogenlike atomic systems (e_P and e_T are the electrons of the projectile and target, respectively) [41]. The finding of Mergel *et al.* [31] is very challenging for atomic scattering theory, since the experimentally estimated behavior $\sigma \sim v^{-7.4\pm 1}$ at $E_P = 0.3$–1.4 MeV of the TI total cross section is at variance with the corresponding prediction v^{-11} of the Thomas classical model [32] as well as the high-energy limit of the peaking Oppenheimer-Brinkman-Kramers second-order (OBK2) approximation [33]. It would be of utmost importance to verify experimentally whether this deviation from the asymptote $\sigma \sim v^{-11}$ would persist at the higher energies at which the asymptotic formulae for the cross section are expected to be more justified than in the interval 0.3–1.4 MeV considered in Ref. [31]. In any case there is an urgent need to theoretically investigate this problem in considerable detail and see whether the TI cross section σ should fall off more slowly than the v^{-11} trend derived from the classical Thomas and the quantal OBK2 approximations. The presently proposed CDW-4B model is well suited to deal with these questions. The present study concentrates on the total cross sections, whereas our subsequent paper will address the question of angular distributions associated with the Thomas P-e-e scattering in the TI. In addition to differential cross sections, it is often very important to acquire information on the impact parameter-dependent transition probability $\mathcal{P}(\vec{\kappa},\rho)$ for, e.g., DI or TI processes. Such a task is not straightforward for ionizing collisions investigated within the RIMS because of the nonuniqueness of the transformation between the transverse momentum transfer $\eta = 2\mu v \sin(\vartheta_P/2)$ and ρ. This problem has recently been studied by Wong *et al.* [42] and investigated further in Ref. [43].

III. CALCULATION OF THE MATRIX ELEMENTS

We consider the heliumlike target in (2.1) as being in the ground state, i.e., $i = {}^1S$ and select the $(1s)^2$ configuration described by the simplest hydrogenic screened one-parameter wave function:

$$\varphi_i'(\vec{x}_1,\vec{x}_2) = N_\lambda^2 e^{-\lambda(x_1+x_2)}, \quad N_\lambda = \sqrt{\frac{\lambda^3}{\pi}}, \tag{3.1}$$

$$\lambda = Z_T - \lambda_S, \quad \lambda_S = \frac{5}{16}.$$

Here, λ_S is the well-known Slater screening and the corresponding binding energy is equal to $-\lambda^2$. It should be noticed that function (3.1) tends to overestimate most cross sections, since the ''outer'' electron is represented by an orbital which is too ''tight.'' In the subsequent analysis, we shall limit ourselves to ground-state capture only, i.e., $f_1=1s$. With the help of the inverse Fourier transform:

$$\frac{1}{\omega}=\frac{1}{2\pi^2}\int\frac{d\vec{\tau}}{\tau^2}\,e^{-i\vec{\tau}\cdot\vec{\omega}}, \tag{3.2}$$

for $\vec{\omega}\in\{\vec{R},\vec{s}_2,\vec{r}_{12}\}$, $\vec{R}=\vec{x}_1-\vec{s}_1$, $\vec{s}_2=\vec{s}_1+\vec{x}_2-\vec{x}_1$, $\vec{r}_{12}=\vec{x}_1-\vec{x}_2$, the transition amplitudes $T_{if}^{\pm}$ can be cast into the following convenient forms:

$$\mathcal{T}_{if}^{-}=\mathcal{T}_R-\mathcal{T}_{s_2}-\mathcal{T}_{\nabla}^{-}+\mathcal{T}_{\varphi_i}^{-}, \tag{3.3}$$

$$\mathcal{T}_{if}^{+}=\mathcal{T}_R-\mathcal{T}_{s_2}+\mathcal{T}_{12}-\mathcal{T}_{x_1}-\mathcal{T}_{\nabla}^{+}, \tag{3.4}$$

where

$$\begin{aligned}\mathcal{T}_R=N_{PT}\frac{Z_P^{5/2}}{2\pi^{5/2}}N_\lambda^2\int\frac{d\vec{\tau}}{\tau^2}\int d\vec{s}_1 e^{i\vec{\alpha}^{+}\cdot\vec{s}_1-Z_P s_1}{}_1F_1(i\nu_P,1,i\upsilon s_1\\ +i\vec{\upsilon}\cdot\vec{s}_1)\int d\vec{x}_1 e^{i\vec{\beta}^{-}\cdot\vec{x}_1-\lambda x_1}{}_1F_1(i\nu_T,1,i\upsilon x_1+i\vec{\upsilon}\cdot\vec{x}_1)\\ \times\int d\vec{x}_2 e^{-i\vec{\kappa}\cdot\vec{x}_2-\lambda x_2}{}_1F_1(i\zeta,1,ipx_2+i\vec{p}\cdot\vec{x}_2),\end{aligned} \tag{3.5}$$

$$\begin{aligned}\mathcal{T}_{s_2}=N_{PT}\frac{Z_P^{5/2}}{2\pi^{5/2}}N_\lambda^2\int\frac{d\vec{\tau}}{\tau^2}\\ \times\int d\vec{s}_1 e^{i\vec{\alpha}^{-}\cdot\vec{s}_1-Z_P s_1}{}_1F_1(i\nu_P,1,i\upsilon s_1+i\vec{\upsilon}\cdot\vec{s}_1)\\ \times\int d\vec{x}_1 e^{i\vec{\beta}^{+}\cdot\vec{x}_1-\lambda x_1}{}_1F_1(i\nu_T,1,i\upsilon x_1+i\vec{\upsilon}\cdot\vec{x}_1)\\ \times\int d\vec{x}_2 e^{-i\vec{\kappa}^{+}\cdot\vec{x}_2-\lambda x_2}{}_1F_1(i\zeta,1,ipx_2+i\vec{p}\cdot\vec{x}_2),\end{aligned} \tag{3.6}$$

$$\begin{aligned}\mathcal{T}_{12}=N_{PT}\frac{Z_P^{3/2}}{2\pi^{5/2}}N_\lambda^2\int\frac{d\vec{\tau}}{\tau^2}\int d\vec{s}_1 e^{i\vec{\alpha}\cdot\vec{s}_1-Z_P s_1}{}_1F_1(i\nu_P,1,i\upsilon s_1\\ +i\vec{\upsilon}\cdot\vec{s}_1)\int d\vec{x}_1 e^{i\vec{\beta}^{-}\cdot\vec{x}_1-\lambda x_1}{}_1F_1(i\nu_T,1,i\upsilon x_1+i\vec{\upsilon}\cdot\vec{x}_1)\\ \times\int d\vec{x}_2 e^{-i\vec{\kappa}^{-}\cdot\vec{x}_2-\lambda x_2}{}_1F_1(i\zeta,1,ipx_2+i\vec{p}\cdot\vec{x}_2),\end{aligned} \tag{3.7}$$

with $\vec{\alpha}^{\pm}=\vec{\alpha}\pm\vec{\tau}$, $\vec{\beta}^{\pm}=\vec{\beta}\pm\vec{\tau}$, $\vec{\kappa}^{\pm}=\vec{\kappa}\pm\vec{\tau}$, and

$$\begin{aligned}\mathcal{T}_{x_1}=N_{PT}\frac{Z_P^{3/2}}{\pi^{1/2}}N_\lambda^2\int d\vec{s}_1 e^{i\vec{\alpha}\cdot\vec{s}_1-Z_P s_1}{}_1F_1(i\nu_P,1,i\upsilon s_1+i\vec{\upsilon}\cdot\vec{s}_1)\\ \times\int d\vec{x}_1\,\frac{e^{i\vec{\beta}\cdot\vec{x}_1-\lambda x_1}}{x_1}\,{}_1F_1(i\nu_T,1,i\upsilon x_1+i\vec{\upsilon}\cdot\vec{x}_1)\\ \times\int d\vec{x}_2 e^{-i\vec{\kappa}\cdot\vec{x}_2-\lambda x_2}{}_1F_1(i\zeta,1,ipx_2+i\vec{p}\cdot\vec{x}_2),\end{aligned} \tag{3.8}$$

$$\begin{aligned}\mathcal{T}_{\nabla}^{+}=N_{PT}\frac{Z_P^{3/2}}{\pi^{1/2}}N_\lambda^2\int d\vec{s}_1 e^{i\vec{\alpha}\cdot\vec{s}_1}{}_1F_1(i\nu_P,1,i\upsilon s_1+i\vec{\upsilon}\cdot\vec{s}_1)\\ \times\vec{\nabla}_{s_1}e^{-Z_P s_1}\cdot\int d\vec{x}_1 e^{i\vec{\beta}\cdot\vec{x}_1-\lambda x_1}\vec{\nabla}_{x_1}{}_1F_1(i\nu_T,1,i\upsilon x_1\\ +i\vec{\upsilon}\cdot\vec{x}_1)\int d\vec{x}_2 e^{-i\vec{\kappa}\cdot\vec{x}_2-\lambda x_2}{}_1F_1(i\zeta,1,ipx_2+i\vec{p}\cdot\vec{x}_2),\end{aligned} \tag{3.9}$$

$$\begin{aligned}\mathcal{T}_{\nabla}^{-}=N_{PT}\frac{Z_P^{3/2}}{\pi^{1/2}}N_\lambda^2\int d\vec{s}_1 e^{i\vec{\alpha}\cdot\vec{s}_1-Z_P s_1}\vec{\nabla}_{s_1}{}_1F_1(i\nu_P,1,i\upsilon s_1\\ +i\vec{\upsilon}\cdot\vec{s}_1)\int d\vec{x}_1 e^{i\vec{\beta}\cdot\vec{x}_1}{}_1F_1(i\nu_T,1,i\upsilon x_1+i\vec{\upsilon}\cdot\vec{x}_1)\cdot\vec{\nabla}_{x_1}\\ \times e^{-\lambda x_1}\int d\vec{x}_2 e^{-i\vec{\kappa}\cdot\vec{x}_2-\lambda x_2}{}_1F_1(i\zeta,1,ipx_2+i\vec{p}\cdot\vec{x}_2).\end{aligned} \tag{3.10}$$

The quantity $\mathcal{T}_{\varphi_i}^{-}$ in Eq. (3.3) is related to the correction term O_{φ_i} from Eqs. (2.26a) and (2.52) due to unavailability of the exact heliumlike wave function. This contribution to the T_{if}^{-} will be practically equal to zero, if we employ the highly correlated variational Hylleraas wave function of Drake [22] or Pekeris [44] for, e.g., He with the corresponding nearly exact binding energy E_i. Such a function φ_i can be considered as exact, but the computation would be prohibitively time-consuming due to a large number of terms containing the r_{12} coordinate. Deferring this for a future study, we shall presently replace the exact wave function by the fully uncorrelated hydrogenic wave function (3.1), i.e., $\varphi_i\simeq\varphi_i'$ and preserve the exact energy E_i in Eq. (2.55) for the prior form, because $O_{\varphi_i'}$ arises only in this version of the T matrix. As a consequence, the corrective term $(E_i-H_{T,\varphi_i})\varphi_i\simeq(E_i-H_{T,\varphi_i'})\varphi_i'$ becomes generally different from zero. Thus, we have

$$\begin{aligned}O_{\varphi_i}&=(E_i-H_{T,\varphi_i})\varphi_i\approx(E_i-H_{T,\varphi_i'})\varphi_i'\\ &=-\left(\frac{1}{r_{12}}-\frac{\lambda_S}{x_1}-\frac{\lambda_S}{x_2}-\Delta E_i\right)\varphi_i'\end{aligned} \tag{3.11}$$

where $\Delta E_i=E_i-E_i'$ and $E_i'=-\lambda^2$. Then, the term $\mathcal{T}_{\varphi_i}^{-}$ can concisely be written as

$$\mathcal{T}_{\varphi_i}^{-}=\mathcal{T}_{12}-\lambda_S(\mathcal{T}_{x_1}+\mathcal{T}_{x_2})-\mathcal{T}_{\Delta}, \tag{3.12}$$

where

$$\mathcal{T}_{x_2}=N_{PT}\,\frac{Z_P^{3/2}}{\pi^{1/2}}\,N_\lambda^2\int d\vec{s}_1 e^{i\vec{\alpha}\cdot\vec{s}_1-Z_P s_1}\,{}_1F_1(i\nu_P,1,ivs_1+i\vec{v}\cdot\vec{s}_1)$$
$$\times\int d\vec{x}_1 e^{i\vec{\beta}\cdot\vec{x}_1-\lambda x_1}\,{}_1F_1(i\nu_T,1,ivx_1+i\vec{v}\cdot\vec{x}_1)$$
$$\times\int d\vec{x}_2\,\frac{e^{-i\vec{\kappa}\cdot\vec{x}_2-\lambda x_2}}{x_2}\,{}_1F_1(i\zeta,1,ipx_2+i\vec{p}\cdot\vec{x}_2),\quad(3.13)$$

$$\mathcal{T}_\Delta=\Delta E_i N_{PT}\,\frac{Z_P^{3/2}}{\pi^{1/2}}\,N_\lambda^2\int d\vec{s}_1 e^{i\vec{\alpha}\cdot\vec{s}_1-Z_P s_1}\,{}_1F_1(i\nu_P,1,ivs_1$$
$$+i\vec{v}\cdot\vec{s}_1)\int d\vec{x}_1 e^{i\vec{\beta}\cdot\vec{x}_1-\lambda x_1}\,{}_1F_1(i\nu_T,1,ivx_1+i\vec{v}\cdot\vec{x}_1)$$
$$\times\int d\vec{x}_2 e^{-i\vec{\kappa}\cdot\vec{x}_2-\lambda x_2}\,{}_1F_1(i\zeta,1,ipx_2+i\vec{p}\cdot\vec{x}_2).\quad(3.14)$$

All the integrals over the electronic coordinates $\vec{x}_1$, $\vec{x}_2$, and $\vec{s}_1$ in Eqs. (3.5)–(3.10), (3.13) and (3.14) can be done analytically by means of the Nordsieck technique [45] with the general results:

$$\int d\vec{r}\,\frac{e^{i\vec{q}\cdot\vec{r}-\lambda r}}{r}\,{}_1F_1(i\nu,1,i\omega r+i\vec{\omega}\cdot\vec{r})$$
$$=\frac{4\pi}{q^2+\lambda^2}\left(1+2\,\frac{\vec{q}\cdot\vec{\omega}-i\lambda\omega}{q^2+\lambda^2}\right)^{-i\nu},\quad(3.15a)$$

$$\int d\vec{r}e^{i\vec{q}\cdot\vec{r}-\lambda r}\,{}_1F_1(i\nu,1,i\omega r+i\vec{\omega}\cdot\vec{r})$$
$$=\frac{8\pi}{q^2+\lambda^2}\left(1+2\,\frac{\vec{q}\cdot\vec{\omega}-i\lambda\omega}{q^2+\lambda^2}\right)^{-i\nu}\left(\lambda\,\frac{1-i\nu}{q^2+\lambda^2}\right.$$
$$\left.+i\nu\,\frac{\lambda-i\nu}{q^2+\lambda^2+2\vec{q}\cdot\vec{\omega}-2i\lambda\omega}\right),\quad(3.15b)$$

$$\int d\vec{r}e^{i\vec{q}\cdot\vec{r}-\lambda r}\vec{\nabla}_r\,{}_1F_1(i\nu,1,i\omega r+i\vec{\omega}\cdot\vec{r})$$
$$=-\nu\omega\,\frac{8\pi}{(q^2+\lambda^2)^2}\left(1+2\,\frac{\vec{q}\cdot\vec{\omega}-i\lambda\omega}{q^2+\lambda^2}\right)^{-i\nu-1}$$
$$\times(\lambda\hat{\vec{\omega}}+i\vec{q}),\quad(3.15c)$$

$$\int d\vec{r}e^{i\vec{q}\cdot\vec{r}}\,{}_1F_1(i\nu,1,i\omega r+i\vec{\omega}\cdot\vec{r})\vec{\nabla}_r e^{-\lambda r}$$
$$=-i\lambda\,\frac{8\pi}{q^2+\lambda^2}\left(1+2\,\frac{\vec{q}\cdot\vec{\omega}-i\lambda\omega}{q^2+\lambda^2}\right)^{-i\nu}\left(\frac{1-i\nu}{q^2+\lambda^2}\,\vec{q}\right.$$
$$\left.+i\nu\,\frac{\vec{q}+\vec{\omega}}{q^2+\lambda^2+2\vec{q}\cdot\vec{\omega}-2i\lambda\omega}\right).\quad(3.15d)$$

This implies:

$$\mathcal{T}_R=\frac{Z_P}{2\pi^2}\,\mathcal{N}\int\frac{d\vec{\tau}}{\tau^2}\,\mathcal{U}_R,\quad \mathcal{T}_{12}=\frac{Z_P}{2\pi^2}\,\mathcal{N}\int\frac{d\vec{\tau}}{\tau^2}\,\mathcal{U}_{12},$$
$$\mathcal{T}_{s_2}=\frac{Z_P}{2\pi^2}\,\mathcal{N}\int\frac{d\vec{\tau}}{\tau^2}\,\mathcal{U}_{s_2},\quad(3.16a)$$

$$\mathcal{T}_\nabla^\pm=\mathcal{N}\mathcal{U}_\nabla^\pm,\quad \mathcal{T}_{x_1}=\mathcal{N}\mathcal{U}_{x_1},\quad \mathcal{T}_\Delta=\mathcal{N}\mathcal{U}_\Delta,\quad \mathcal{T}_{x_2}=\mathcal{N}\mathcal{U}_{x_2},\quad(3.16b)$$

where

$$\mathcal{N}=N_\lambda^2 N_{PT}(8\pi)^3\sqrt{\frac{Z_P^3}{\pi}},\quad(3.17)$$

$$\mathcal{U}_R=\frac{T_+^{i\nu_P}R_-^{i\nu_T}S_0^{i\zeta}\mathcal{A}\mathcal{L}_0}{(\alpha_+\beta_-\kappa_0)^2},\quad \mathcal{U}_{s_2}=\frac{T_-^{i\nu_P}R_+^{i\nu_T}S_+^{i\zeta}\mathcal{B}\mathcal{L}_+}{(\alpha_-\beta_+\kappa_+)^2},\quad(3.18)$$

$$\mathcal{U}_\Delta=\Delta E_i\,\frac{T_0^{i\nu_P}R_0^{i\nu_T}S_0^{i\zeta}\mathcal{D}\mathcal{L}_0}{(\alpha_0\beta_0\kappa_0)^2},\quad \mathcal{U}_{x_2}=\frac{T_0^{i\nu_P}R_0^{i\nu_T}S_0^{i\zeta}\mathcal{D}}{2(\alpha_0\beta_0)^2\kappa_0},\quad(3.19)$$

$$\mathcal{U}_{12}=\frac{1}{Z_P}\,\frac{T_0^{i\nu_P}R_-^{i\nu_T}S_i^{i\zeta}\mathcal{C}\mathcal{L}_-}{(\alpha_0\beta_-\kappa_-)^2},\quad(3.20)$$

$$\mathcal{U}_\nabla^-=i\lambda v\,\nu_P$$
$$\times\frac{T_0^{i\nu_P+1}R_0^{i\nu_T}S_0^{i\zeta}[\vec{\beta}(1-i\nu_T)-i\nu_T\vec{\alpha}R_0](Z_P\hat{\vec{v}}+i\vec{\alpha})\mathcal{L}_0}{(\alpha_0\beta_0\kappa_0)^2},\quad(3.21)$$

$$\mathcal{U}_\nabla^+=iZ_P v\,\nu_T$$
$$\times\frac{T_0^{i\nu_P}R_0^{i\nu_T+1}S_0^{i\zeta}[\vec{\alpha}(1-i\nu_P)-i\nu_P\vec{\beta}T_0](\lambda\hat{\vec{v}}+i\vec{\beta})\mathcal{L}_0}{(\alpha_0\beta_0\kappa_0)^2},\quad(3.22)$$

$$\mathcal{U}_{x_1}=\frac{T_0^{i\nu_P}R_0^{i\nu_T}S_0^{i\zeta}[Z_P(1-i\nu_P)+i\nu_P(Z_P-iv)T_0]\mathcal{L}_0}{2\beta_0(\alpha_0\kappa_0)^2},\quad(3.23)$$

and

$$\mathcal{A}=[Z_P(1-i\nu_P)+i\nu_P(Z_P-iv)T_+]$$
$$\times[\lambda(1-i\nu_T)+i\nu_T(\lambda-iv)R_-],\quad(3.24a)$$

$$\mathcal{B}=[Z_P(1-i\nu_P)+i\nu_P(Z_P-iv)T_-]$$
$$\times[\lambda(1-i\nu_T)+i\nu_T(\lambda-iv)R_+],\quad(3.24b)$$

$$\mathcal{C}=[Z_P(1-i\nu_P)+i\nu_P(Z_P-iv)T_0]$$
$$\times[\lambda(1-i\nu_T)+i\nu_T(\lambda-iv)R_-],\quad(3.24c)$$

$$\mathcal{D}=[Z_P(1-i\nu_P)+i\nu_P(Z_P-iv)T_0]$$
$$\times[\lambda(1-i\nu_T)+i\nu_T(\lambda-iv)R_0],\quad(3.24d)$$

with

$$T_{\pm}^{-1}=1+2\frac{\vec{\alpha}^{\pm}\cdot\vec{v}-iZ_P v}{\alpha_{\pm}},\quad T_0^{-1}=1+2\frac{\vec{\alpha}\cdot\vec{v}-iZ_P v}{\alpha_0},\tag{3.25}$$

$$R_{\pm}^{-1}=1+2\frac{\vec{\beta}^{\pm}\cdot\vec{v}-i\lambda v}{\beta_{\pm}},\quad R_0^{-1}=1+2\frac{\vec{\beta}\cdot\vec{v}-i\lambda v}{\beta_0},\tag{3.26}$$

$$S_{\pm}^{-1}=1-2\frac{\vec{\kappa}^{\pm}\cdot\vec{p}+i\lambda p}{\kappa_{\pm}},\quad S_0^{-1}=1-2\frac{\vec{\kappa}\cdot\vec{p}+i\lambda p}{\kappa_0},\tag{3.27}$$

$$\alpha_{\pm}=(\alpha^{\pm})^2+Z_P^2,\quad \beta_{\pm}=(\beta^{\pm})^2+\lambda^2,\quad \kappa_{\pm}=(\kappa^{\pm})^2+\lambda^2,\tag{3.28}$$

$$\alpha_0=\alpha^2+Z_P^2,\quad \beta_0=\beta^2+\lambda^2,\quad \kappa_0=\kappa^2+\lambda^2,\tag{3.29}$$

$$\mathcal{L}_{\pm}=\lambda(1-i\zeta)+i\zeta(\lambda-ip)S_{\pm},$$

$$\mathcal{L}_0=\lambda(1-i\zeta)+i\zeta(\lambda-ip)S_0.\tag{3.30}$$

This completes the analytical part of the calculation, so that the prior σ_{if}^{-} and the post σ_{if}^{+} forms of the total cross sections can be succinctly summarized as follows:

$$\sigma_{if}^{-}(\pi a_0^2)=\mathcal{N}'\int d\vec{\kappa}\; n_\zeta \times\int_0^\infty d\eta\;\eta|\mathcal{F}^{-}-\mathcal{U}_{\nabla}^{-}-\lambda_S(\mathcal{U}_{x_1}+\mathcal{U}_{x_2})-\mathcal{U}_{\Delta}|^2,\tag{3.31}$$

$$\sigma_{if}^{+}(\pi a_0^2)=\mathcal{N}'\int d\vec{\kappa}\; n_\zeta\int_0^\infty d\eta\;\eta|\mathcal{F}^{+}-\mathcal{U}_{\nabla}^{+}-\mathcal{U}_{x_1}|^2,\tag{3.32}$$

where

$$\mathcal{F}^{-}=\mathcal{F}^{+}=\frac{Z_P}{2\pi^2}\int\frac{d\vec{\tau}}{\tau^2}(\mathcal{U}_R-\mathcal{U}_{s_2}+\mathcal{U}_{12}),\tag{3.33}$$

$$\mathcal{N}'=\frac{2^{14}}{v^2}N_\lambda^4 Z_P^3\pi^2\nu_P\nu_T\frac{e^{\pi(\nu_P+\nu_T)}}{\sinh(\pi\nu_P)\sinh(\pi\nu_T)},\quad n_\zeta=\frac{\pi\zeta e^{\pi\zeta}}{\sinh(\pi\zeta)}.\tag{3.34}$$

The integrations over $\vec{\kappa}=(\kappa\sin\theta_\kappa\cos\phi_\kappa,\kappa\sin\theta_\kappa\sin\phi_\kappa,\kappa\cos\theta_\kappa)$, $\vec{\tau}=(\tau\sin\theta_\tau\cos\phi_\tau,\tau\sin\theta_\tau\sin\phi_\tau,\tau\cos\theta_\tau)$, and η have to be performed numerically. Hence, the final expressions (3.31) and (3.32) for the total cross sections for the process (2.1) in the present CDW-4B method are given in terms of the above seven-dimensional (7D) integrals over the real variables $\kappa\in[0,\infty]$, $\theta_\kappa\in[0,\pi]$, $\phi_\kappa\in[0,2\pi]$, $\eta\in[0,\infty]$, $\tau\in[0,\infty]$, $\theta_\tau\in[0,\pi]$, and $\phi_\tau\in[0,2\pi]$. The TCDW-IEM method of Ref. [10] also encounters similar 7D scattering integrals when dealing with the total cross sections for the TI process (2.1). In Dunseath and Crothers' TCDW-IEM model [10] the Pluvinage wave function [14] is employed with explicit allowance for the r_{12} coordinate. This could be done in the present CDW-4B theory, as well.

IV. RESULTS

The integrations over ϕ_κ and ϕ_τ are performed easily by means of the very simple and highly efficient Gauss-Mehler (GM) quadrature:

$$\int_0^{2\pi}d\phi\; f(\cos\phi)=\frac{2\pi}{N_{\rm GM}}\sum_{k=1}^{N_{\rm GM}}f\left(\cos\frac{2k-1}{2N_{\rm GM}}\pi\right),\tag{4.1}$$

where $N_{\rm GM}$ is the number of the pivotal points. The remaining integrals over θ_κ, θ_τ, κ, τ, and η are carried out after a change of the variables according to

$$\cos\theta_\kappa=u,\quad \cos\theta_\tau=v,\quad u\in[-1,+1],\quad v\in[-1,+1],\tag{4.2}$$

$$\kappa=\sqrt{\frac{2(1+x)}{1-x}},\quad x\in[-1,+1],$$

$$\tau=\frac{1+\xi}{1-\xi},\quad \xi\in[-1,+1],\tag{4.3}$$

$$\eta=\sqrt{\frac{2(1+z)}{1-z}},\quad z\in[-1,+1].\tag{4.4}$$

Then, the variable-order Gauss-Legendre (GL) routines are applied to the u, v, x, ξ, and z integrations following the rule:

$$\int_0^\pi d\vartheta\;\sin\vartheta f(\cos\vartheta)=\sum_{k=1}^{N_{\rm GL}}w_k f(x_k),\tag{4.5}$$

where x_k are the zeros of the Legendre polynomials and w_k are the associated weights. The change of the variable η through Eq. (4.4) is particularly important, because it concentrates the integration points in a narrow forward cone, which contributes dominantly to the total cross sections [46]. The orders of the GM and GL quadratures, i.e., the numbers $N_{\rm GM}$ and $N_{\rm GL}$ of the pivotal points are varied until convergence to *two decimal places* is obtained for the total cross sections. In practice, only $N_{\rm GM}\leqslant 20$ for the ϕ_κ, ϕ_τ integrals and $N_{\rm GL}\leqslant 40$ for the remaining θ_κ, θ_τ, κ, τ, η quadratures proved to be sufficient. The expressions in Eqs. (4.3) and (4.4) are not used directly due to an apparent overflow at $x\approx 1$, $\xi\approx 1$, and $z\approx 1$. This difficulty is readily avoided by scaling the whole integrand analytically, i.e., by factoring out the terms $1/\sqrt{1-x}$, $1/(1-\xi)$, and $1/\sqrt{1-z}$ from the whole integrand which, in turn, becomes a smooth function throughout the entire integration manifold. Finally, this algorithm is subjected to a powerful vectorization, with at least two orders of magnitude saving in the computer-central-processing time.

As an illustration of the proposed CDW-4B approximation, the total cross sections are computed for the following symmetric transfer ionization:

$$\mathrm{He}^{2+}+\mathrm{He}(1s^2)\rightarrow\mathrm{He}^{+}(1s)+\mathrm{He}^{2+}+e.\tag{4.6}$$

The computations are carried out for both the prior σ_{if}^{-} and post σ_{if}^{+} total cross sections at impact energies ranging from 30 to 1000 keV/amu. The results are displayed in Tables I–III and Figs. 1–4. In Fig. 1, a comparison is made between

TABLE I. The ''prior'' total cross sections σ_{if}^{-} (cm^2) in the CDW-4B model as a function of the laboratory incident energy E (keV/amu) for transfer ionization reaction: $^4He^{2+}+{}^4He(1s^2)\rightarrow{}^4He^{+}(1s)+{}^4He^{2+}+e$. The columns labeled by $\sigma_{if}^{-(a)}$ and $\sigma_{if}^{-(b)}$ correspond to the results obtained with and without the approximation $V_P(R,s_2)\equiv Z_P(1/R-1/s_2)\approx 0$, respectively (see text). The notation $x.yz[-uu']$ implies $x.yz\times 10^{-uu'}$.

E (keV/amu)	$\sigma_{if}^{-(a)}$ (cm^2)	$\sigma_{if}^{-(b)}$ (cm^2)
30	3.95 [−17]	5.21 [−17]
40	3.23 [−17]	3.79 [−17]
50	2.84 [−17]	3.12 [−17]
60	2.58 [−17]	2.72 [−17]
70	2.36 [−17]	2.43 [−17]
80	2.16 [−17]	2.19 [−17]
90	1.97 [−17]	1.98 [−17]
100	1.79 [−17]	1.78 [−17]
125		1.37 [−17]
130	1.33 [−17]	
145	1.14 [−17]	
150		1.05 [−17]
165	9.29 [−18]	
175		8.02 [−17]
180	7.95 [−18]	
200	6.46 [−18]	6.13 [−18]
250	3.89 [−18]	3.64 [−18]
300	2.40 [−18]	2.22 [−18]
400	9.85 [−19]	8.92 [−19]
500	4.46 [−19]	3.98 [−19]
600	2.20 [−19]	1.93 [−19]
700	1.16 [−19]	
750		7.46 [−20]
800	6.52 [−20]	
900	3.84 [−20]	
1000	2.36 [−20]	1.99 [−20]

TABLE II. The ''prior'' total cross sections σ_{if}^{-} (cm^2) in the CDW-4B as a function of the laboratory incident energy E (keV/amu) for transfer ionization reaction: $^4He^{2+}+{}^4He(1s^2)\rightarrow{}^4He^{+}(1s)+{}^4He^{2+}+e$. The columns labeled by $\sigma_{if}^{-(c)}$ and $\sigma_{if}^{-(d)}$ correspond to the results obtained with and without the term $O_{\varphi_i'}\equiv O_i$, respectively (see text).

E (keV/amu)	$\sigma_{if}^{-(c)}$ (cm^2)	$\sigma_{if}^{-(d)}$ (cm^2)
30	4.91 [−17]	5.21 [−17]
40	3.63 [−17]	3.79 [−17]
50	3.00 [−17]	3.12 [−17]
70	2.33 [−17]	2.43 [−17]
100	1.71 [−17]	1.78 [−17]
150	1.02 [−17]	1.05 [−17]
200	2.95 [−18]	6.13 [−18]
500	3.88 [−19]	3.98 [−19]
700	9.92 [−20]	
1000	2.00 [−20]	1.99 [−20]

TABLE III. The ''post'' σ_{if}^{+} (cm^2) and the ''prior'' σ_{if}^{-} (cm^2) total cross sections in the CDW-4B model as a function of the laboratory incident energy E (keV/amu) for transfer ionization reaction: $^4He^{2+}+{}^4He(1s^2)\rightarrow{}^4He^{+}(1s)+{}^4He^{2+}+e$.

E (keV/amu)	σ_{if}^{+} (cm^2)	σ_{if}^{-} (cm^2)
30	9.32 [−17]	5.21 [−17]
35		4.35 [−17]
40	7.40 [−17]	3.79 [−17]
45		3.40 [−17]
50	5.96 [−17]	3.12 [−17]
55		2.90 [−17]
60	4.83 [−17]	2.72 [−17]
65		2.57 [−17]
70	3.95 [−17]	2.43 [−17]
75		2.30 [−17]
80	3.24 [−17]	2.19 [−17]
85		2.08 [−17]
90	2.67 [−17]	1.98 [−17]
95		1.88 [−17]
100	2.22 [−17]	1.78 [−17]
125	1.42 [−17]	1.37 [−17]
150	9.43 [−18]	1.05 [−17]
175		8.02 [−18]
200	4.48 [−18]	6.13 [−18]
250	2.32 [−18]	3.64 [−18]
300	1.30 [−18]	2.22 [−18]
350		1.39 [−18]
400	4.75 [−19]	8.92 [−19]
500	2.05 [−19]	3.98 [−19]
600		1.93 [−19]
750	3.98 [−20]	7.46 [−20]
1000	1.16 [−20]	1.99 [−20]

the prior cross sections $\sigma_{if}^{-(a)}$ and $\sigma_{if}^{-(b)}$ of the CDW-4B model *with* and *without* the approximation $1/R=1/s_2$ corresponding to $V_P(R,s_2)=0$ and $V_P(R,s_2)\neq 0$, respectively, as stated in Eq. (2.66). It is seen from Table I and Fig. 1 that the potential $V_P(R,s_2)$ contributes by some 24% at low and 16% at high energies. At lower impact energies, where the present theory is not expected to be adequate, the probability for the TI is enhanced by inclusion of the interaction $V_P(R,s_2)=Z_P(1/R-1/s_2)$. At high energies, which are more appropriate for the CDW-4B method, this pattern is reversed and $V_P(R,s_2)$ tends to suppress the chance for the TI. As discussed before, the potential $-Z_P/s_2$ from $V_P(R,s_2)$ causes the capture of e_1 through the inherent e_1-e_2 subinteraction. Therefore, the situation observed in Fig. 1 indicates that the dynamic electron correlation could play an important role at high impact energies (see also Table I).

Further, we have evaluated the contribution of the term $O_{\varphi_i'}\equiv(E_i-H_{T,\varphi_i'})\varphi_i'$, which is contained only in the prior cross section. Namely, if we ignore this term in Eq. (2.52), we would end up with the formula:

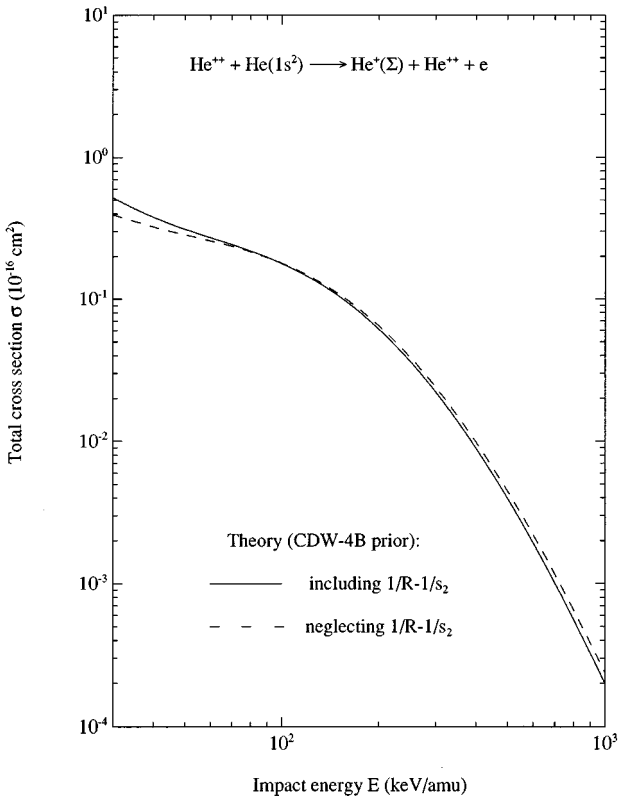

FIG. 1. The total cross sections as a function of the laboratory incident energy E (keV/amu) for the reaction: $^4He^{2+}+{}^4He(1s^2)\rightarrow{}^4He^+(1s)+{}^4He^{2+}+e$. The dashed and the full lines represent the ''prior'' cross sections $\sigma_{if}^{-(a)}$ and $\sigma_{if}^{-(b)}$ of the CDW-4B approximation with and without the approximation $V_P(R,s_2)\equiv Z_P(1/R-1/s_2)\approx 0$, respectively (see also Table I).

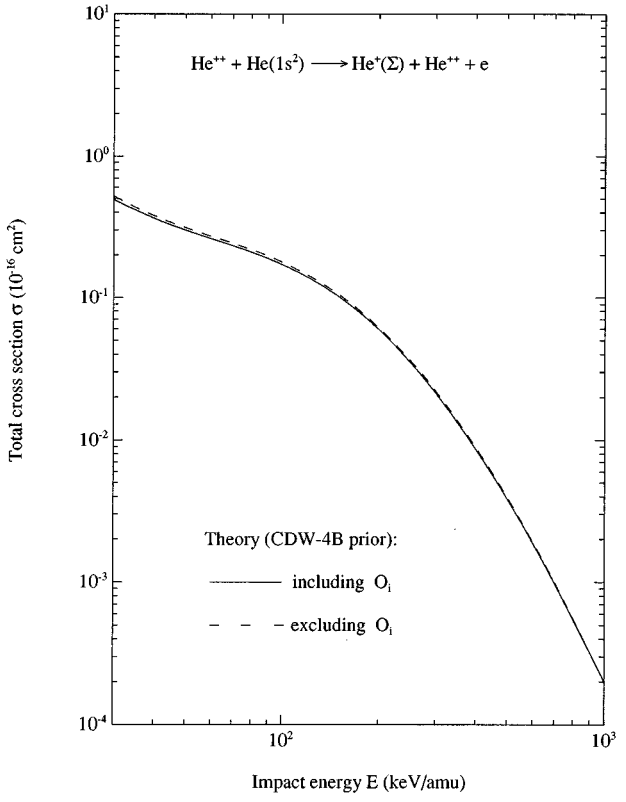

FIG. 2. The total cross sections as a function of the laboratory incident energy E (keV/amu) for the reaction: $^4He^{2+}+{}^4He(1s^2)\rightarrow{}^4He^+(1s)+{}^4He^{2+}+e$. The full and the dashed lines represent, respectively, the ''prior'' cross sections $\sigma_{if}^{-(c)}$ and $\sigma_{if}^{-(d)}$ of the CDW-4B method with and without the initial-eigenvalue corrective term $O_i\equiv O_{\varphi_i'}=(E_i-H_{T,\varphi_i'})\varphi_i'$ from Eqs. (2.52) and (3.11) (see Table II).

$$\sigma_{if}^{-}(\pi a_0^2)=\mathcal{N}'\int d\vec{k}\; n_\zeta\int_0^\infty d\eta\;\eta|\mathcal{F}^{-}-\mathcal{U}_\nabla^{-}|^2,$$
$$\mathcal{F}^{-}=\frac{Z_P}{2\pi^2}\int\frac{d\vec{\tau}}{\tau^2}\,(\mathcal{U}_R-\mathcal{U}_{s_2}), \tag{4.7}$$

instead of having Eq. (3.31). The numerical results of such a version are shown in Table II, where $\sigma_{if}^{-(c)}$ and $\sigma_{if}^{-(d)}$ denote the prior total cross section *with* and *without* the term $O_{\varphi_i'}$, respectively. The results for both $\sigma_{if}^{-(c)}$ and $\sigma_{if}^{-(d)}$ are displayed also in Fig. 2. As can be seen from this figure, the cross sections $\sigma_{if}^{-(c)}$ and $\sigma_{if}^{-(d)}$ are quite close to each other and their difference is slightly more pronounced at lower and intermediate than at high energies. In the absolute magnitude, however, this difference does not exceed 6% and the values of the ratio $\sigma_{if}^{-(d)}/\sigma_{if}^{-(c)}$ are all contained in the interval [0.995,1.061] at the energies under study (see Table II). Thus, it follows that the term $O_{\varphi_i'}$ does not contribute significantly to the total cross section, when φ_i' from Eq. (3.1) is used. A similar conclusion has recently been reached in Ref. [27] for the DC within the CB1-4B model.

Next, we examine the so-called ''post-prior'' discrepancy, which arises from unequal perturbation potentials in the T matrices (2.52) and (2.56). In Fig. 3, we depict the ''prior'' σ_{if}^{-} and ''post'' σ_{if}^{+} cross sections of the CDW-4B approximation. Here, the prior results do not include the correction $O_{\varphi_i'}$, which is shown above to be negligibly small. Hence, the difference between σ_{if}^{-} and σ_{if}^{+} is solely due to the potential $V(r_{12},x_1)=1/r_{12}-1/x_1$, which is present in the post and absent from the prior cross sections. An inspection of Fig. 3 reveals that the post-prior discrepancy is very significant throughout the energy range 30–1000 keV/amu. The post cross sections are larger by about 45% than the prior results at lower energies, with precisely the opposite pattern at higher energies. Such a considerable difference can be attributed to the role of the dielectronic repulsion $1/r_{12}$. Except for a much larger difference, this qualitative behavior is reminiscent of the situation described before in Fig. 1, where we compared the results with and without the correlation term $1/R-1/s_2$ in the prior version of the CDW-4B model. In the same Fig. 3, the experimental data of Shah *et al.* [6] are also displayed. In contrast to the prior variant σ_{if}^{-}, the post version σ_{if}^{+} of the CDW-4B method is found to be in satisfactory agreement with the measurements at impact energies $E\geqslant 80$ keV/amu. At lower energies, the results for σ_{if}^{+} are larger than the experimental values, which is expected since the CDW-4B is a high-energy approximation. This is consistent with the previously assessed lower energy limit of validity of the CDW-3B and CDW-4B approximations for single charge exchange in the processes (2.65) and (2.69). In Sec. III, we already identified the reason for which one should expect superiority of the post over the prior version of

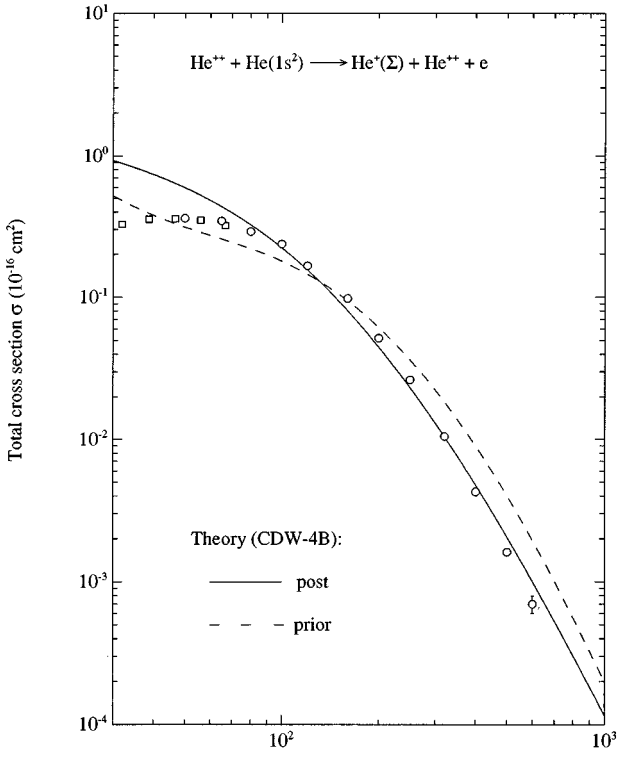

FIG. 3. The total cross sections as a function of the laboratory incident energy E (keV/amu) for the reaction: $^4He^{2+}+{}^4He(1s^2)\rightarrow{}^4He^+(1s)+{}^4He^{2+}+e$. The full and the dashed lines represent, respectively, the ''post'' σ_{if}^{+} and the ''prior'' σ_{if}^{-} cross sections of the CDW-4B model. Experimental data: □, ○ Shah *et al.* [6].

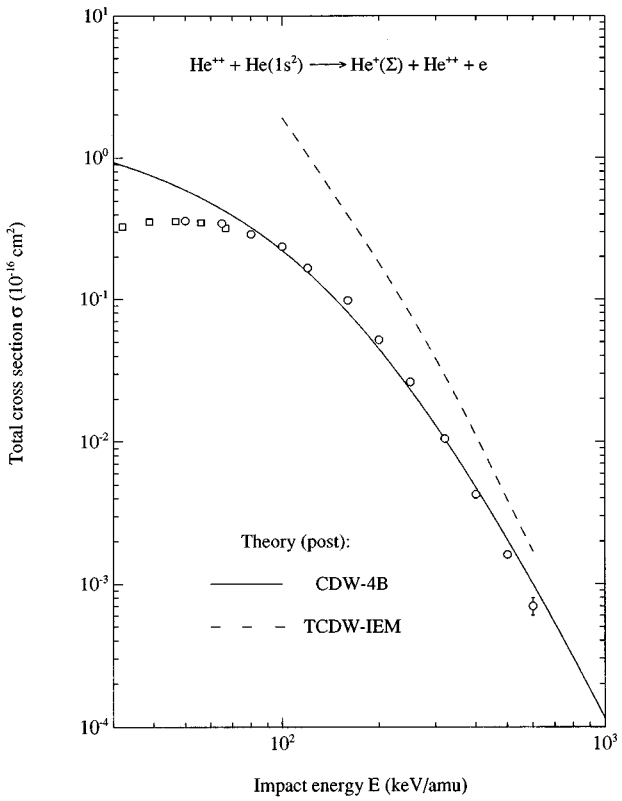

FIG. 4. The total cross sections as a function of the laboratory incident energy E (keV/amu) for the transfer ionization: $^4He^{2+}+{}^4He(1s^2)\rightarrow{}^4He^+(1s)+{}^4He^{2+}+e$. The full line represents the ''post'' total cross section σ_{if}^{+} of the CDW-4B method. The dashed line represents the corresponding ''post'' cross sections of the TCDW-IEM due to Dunseath and Crothers [10]. Experimental data: □,○ Shah *et al.* [6].

the CDW-4B method. This reason was precisely the *direct* appearance of the electron-electron interaction $1/r_{12}$ in the perturbation U_f of the post form as indicated in (2.62). The interelectronic potential $1/r_{12}$ also appears in U_i of the prior form, but in an indirect way through the object $(E_i-H_{T,\varphi_i'})\varphi_i'=-[1/r_{12}-(\lambda_S/x_1+\lambda_S/x_2+\Delta E_i)]\varphi_i'$, which is invoked in Eq. (2.61) as a consequence of replacing the exact wave function $\varphi_i(\vec{x}_1,\vec{x}_2)$ by Eq. (3.1). However, after such a replacement, the three terms $-(\lambda_S/x_1+\lambda_S/x_2+\Delta E_i)$ appear to largely cancel the contribution from $1/r_{12}$. In this way, the whole effect of the electronic correlation was practically washed out from T_{if}^{-}.

In Fig. 4, comparison is given between the TCDW-IEM of Dunseath and Crothers [10] and our CDW-4B method. Both approximations are taken in the same post version. The TCDW-IEM includes the static electron correlation (SEC) in the target through the bound state wave function of the Pluvinage type [14]:

$$\varphi_i(\vec{x}_1,\vec{x}_2)\approx\varphi_i''(\vec{x}_1,\vec{x}_2)$$
$$=c(k)\,\frac{Z_T^3}{\pi}\,e^{-Z_T(x_1+x_2)}e^{-ikr_{12}}$$
$$\times{}_1F_1(1-i\eta',2,2ikr_{12}),\qquad(4.8)$$

where $r_{12}=|\vec{x}_1-\vec{x}_2|$, $\eta'=1/(2k)$, and $c(k)$ is the normalization constant. Here, k is a nonlinear variational parameter. The corresponding lowest binding energy $E_{i,\mathrm{Pluv}}=-2.878$ for the ground state $i={}^1S$ of helium is obtained for $k=0.41$, in which case $c(k)=0.603\,366$. The wave function (4.8) contains two entirely uncorrelated hydrogenic wave functions with the *unscreened* charge Z_T multiplied with a corrective r_{12}-dependent term of the form $\exp(-ikr_{12}){}_1F_1(1-i\eta',2,2ikr_{12})$. By definition, the exact total correlation energy $E_{i,\mathrm{ex}}^{(\mathrm{tot.\ corr})}$ is introduced as the difference $E_{i,\mathrm{ex}}-E_{i,\mathrm{RHF}}$ between the exact $E_i\equiv E_{i,\mathrm{ex}}$ (Drake [22], Pekeris [44], or an experimental data) and the corresponding self-consistent field Roothan-Hartree-Fock (RHF) value $E_{i,\mathrm{RHF}}$. The quantity $E_{i,\mathrm{ex}}^{(\mathrm{tot.\ corr})}$ includes both radial and angular correlations. In the case of helium, $E_{i,\mathrm{ex}}=-2.903\,724\,4$, $E_{i,\mathrm{RHF}}=-2.861\,67$ and, therefore, $E_{i,\mathrm{ex}}^{(\mathrm{tot.\ corr})}=-0.042\,504\,4$. The Pluvinage total (radial and angular) correlation energy $E_{i,\mathrm{Pluv}}^{(\mathrm{tot.\ corr})}=E_{i,\mathrm{Pluv}}-E_{i,\mathrm{RHF}}=-0.016\,33$ amounts for 38.4% of the exact total correlation energy $E_{i,\mathrm{ex}}^{(\mathrm{tot.\ corr})}$. For comparison, a much simpler four-parameter wave function of Boham and Kohl [47] for helium given by:

$$\varphi_i(\vec{x}_1,\vec{x}_2)\approx\varphi_i^{BK}(\vec{x}_1,\vec{x}_2)=N_{BK}(e^{-a_1x_1-a_2x_2}+e^{-a_2x_1-a_1x_2})$$
$$\times(1+a_3e^{-a_4r_{12}}),\qquad(4.9)$$

yields the binding energy $E_i(BK)=-2.901\,923$ and provides remarkable 94.7% of $E_{i,\mathrm{ex}}^{(\mathrm{tot.corr})}$. Even neglecting the non-linear term $a_3e^{-a_4r_{12}}$ in (4.9), i.e., including solely the

radial correlations, in which case one recovers the two-parameter Eckart-Silverman wave function for the $(1s,1s')$ configuration [48]:

$$\varphi_i(\vec{x}_1,\vec{x}_2)\approx\varphi_i^{\mathrm{ES}}(\vec{x}_1,\vec{x}_2)=N_{\mathrm{ES}}(e^{-a_1x_1-a_2x_2}+e^{-a_2x_1-a_1x_2}), \tag{4.10}$$

implies: $E_{i,\mathrm{ES}}=-2.875\,661\,4$. Such a result amounts for 32.9% of $E_{i,\mathrm{ex}}^{(\mathrm{tot.\ corr})}$ and this is very close to the corresponding Pluvinage estimate obtained with Eq. (4.8). Use of Eqs. (4.9) and (4.10) in scattering problems is quite straightforward. In contrast, Eq. (4.8) requires a considerable computational effort with bound-free atomic form factors through numerical quadratures for the Laplace transforms in a complex plane [10]. In the TCDW-IEM, the dynamic electron correlations (DEC) are neglected altogether. The CDW-4B model explicitly includes the DEC through the dielectronic interaction $1/r_{12}$ in the transition T operator. The SEC can also be fully included in the CDW-4B, but it is ignored in the present illustration with purpose of providing an unambiguous assessment of the DEC alone. The relative role of the SEC and the DEC could otherwise be inferred from the two curves associated with the TCDW-IEM and CDW-4B displayed in Fig. 4. The DEC emerges as more important than the SEC. When comparing these two theories with the experimental data in Fig. 4, it is seen that the CDW-4B represents a substantial improvement over the TCDW-IEM. This seems to indicate that only four-body theories, with a proper inclusion of the *dynamic* electronic correlations, could successfully describe transfer ionization (4.6).

V. CONCLUSION

We have investigated the problem of transfer ionization in collisions between bare nuclei and heliumlike atomic systems. A second-order theory, termed the four-body continuum distorted-wave (CDW-4B) method, is formulated. The scattering wave functions of the proposed method exhibit the proper asymptotic behaviors in both entrance and exit channels. The CDW-4B approximation is presently applied to the transfer ionization in symmetric collisions between α particles and helium targets at impact energies from 30 to 1000 keV/amu. The previous independent electron model (TCDW-IEM) is known to largely overestimate the experimental data. The conclusion from the present study indicates that the dynamic electronic correlations in the active perturbation potentials are much more important than the static ones in the target bound state wave function. Agreement of the theoretical total cross sections obtained by means of the CDW-4B model with the available measured findings is very good. Such a substantial improvement over the CDW-IEM is attributed solely to the dynamic electron correlation effects.

ACKNOWLEDGMENTS

This work was supported by the Wenner-Gren Science Foundation (Stockholm, Sweden). The authors also appreciate useful discussions with A. Salin, R. Gayet, R. Rivarola, J. Hansen, A. Bárány, R. Schuch, H. Schmidt-Böcking, and R. Dörner.

[1] J. A. Tanis, Nucl. Instrum. Methods Phys. Res. Sect. B **62**, 52 (1987); J. A. Tanis, M. W. Clark, R. Price, S. M. Ferguson, and R. E. Olson, *ibid*. **23**, 167 (1987); J. Tanis, E. M. Bernstein, M. Clark, W. G. Graham, R. H. McFarland, T. J. Morgan, B. M. Johnson, K. W. Jones, and M. Meron, Phys. Rev. Lett. **31**, 4040 (1985); J. A. Tanis, G. Schiwietz, D. Schneider, N. Stolterfoht, W. G. Graham, H. Altevogt, R. Kowallik, A. Mattis, B. Skogvall, T. Schneider, and E. Szmola, Phys. Rev. A **39**, 1571 (1989).

[2] L. H. Andersen, M. Frost, P. Hvelplund, and H. Knudsen, Phys. Rev. Lett. **52**, 518 (1984); H. Damsgaard, H. K. Haugen, P. Hvelplund, and H. Knudsen, Phys. Rev. A **27**, 112 (1983); H. Knudsen, L. H. Andersen, P. Hvelplund, J. Sorensen, and D. Ćirić, J. Phys. B **20**, L253 (1987).

[3] S. Datz, R. Hippler, L. H. Andersen, P. F. Dittner, H. Knudsen, H. F. Krause, P. D. Miller, P. L. Pepmiller, T. Rosseel, and R. Schuch, Phys. Rev. A **41**, 3559 (1990).

[4] R. Schuch, E. Justiniano, H. Vogt, G. Deco, and N. Grün, J. Phys. B **24**, L133 (1991).

[5] N. V. de Castro Faria, F. L. Freire, Jr., and A. G. de Pinho, Phys. Rev. A **37**, 280 (1988); J. L. Shingpaugh, J. M. Sanders, J. M. Hall, D. H. Lee, H. Schmidt-Böcking, T. N. Tripping, T. J. M. Zouros, and P. Richard, *ibid*. **45**, 2922 (1992).

[6] M. B. Shah and H. B. Gilbody, J. Phys. B **18**, 899 (1985); M. B. Shah, P. McCllion, and H. B. Gilbody, J. Phys. B **22**, 3037 (1989); V. V. Afrosimov, G. A. Leiko, Yu. A. Mamaev, and M. N. Panov, Zh. Eksp. Teor. Fiz. **67**, 1239 (1974) [Sov. Phys. JETP **38**, 243 (1974)].

[7] E. Horsdal, B. Jensen, and K. O. Nielsen, Phys. Rev. Lett. **57**, 1414 (1986).

[8] J. Pálinkás, R. Schuch, H. Cederquist, and O. Gustafsson, Phys. Rev. Lett. **63**, 2464 (1989); Phys. Scr. **42**, 175 (1990).

[9] G. Deco and N. Grün, Z. Phys. D **18**, 339 (1991).

[10] K. M. Dunseath and D. S. F. Crothers, J. Phys. B **24**, 5003 (1991); N. C. Deb and D. S. F. Crothers, *ibid*. **23**, L799 (1990); **24**, 2359 (1991); D. P. Marshall, C. Le Sech, and D. S. F. Crothers, *ibid*. **26**, L219 (1993).

[11] D. S. F. Crothers and R. McCarroll, J. Phys. B **20**, 2835 (1987).

[12] R. Shingal and C. D. Lin, J. Phys. B **24**, 251 (1991).

[13] V. A. Sidorovich, V. S. Nikolaev, and J. H. McGuire, Phys. Rev. A **31**, 2193 (1985); M. Ghosh, C. R. Mandal, and S. C. Mukherjee, J. Phys. B **18**, 3797 (1985); Phys. Rev. A **35**, 5259 (1987).

[14] P. Pluvinage, Ann. Phys. (N.Y.) **5**, 145 (1950); J. Phys. Radium **12**, 789 (1951).

[15] Dž. Belkić and Mančev I, Phys. Scr. **45**, 35 (1992); **46**, 18 (1993).

[16] Dž. Belkić, Nucl. Instrum. Methods Phys. Res. Sect. B **86**, 62 (1994).

[17] R. Gayet, J. Hanssen, L. Jacqui, A. Martinez, and R. Rivarola, Phys. Scr. **53**, 549 (1996).

[18] J. F. Reading and A. L. Ford, J. Phys. B **20**, 3747 (1987); J. F. Reading, K. A. Hall, and A. L. Ford, *ibid*. **26**, 3549 (1993).

[19] H. Bachau, R. Gayet, J. Hanssen, and A. Zerarka, J. Phys. B

25, 839 (1992); R. Gayet, J. Hanssen, and L. Jacqui, *ibid*. **28**, 2193 (1995).
[20] D. Brandt, Phys. Rev. A **27**, 1314 (1983).
[21] S. Bhattacharyya, K. Rinn, E. Salzborn, and L. Chatterjee, J. Phys. B **21**, 111 (1988); S. N. Chatterjee, S. Prasad, and B. N. Roy, *ibid*. **21**, 1209 (1988).
[22] G. W. F. Drake, Nucl. Instrum. Methods Phys. Res. Sect. B **31**, 7 (1988).
[23] I. M. Cheshire, Proc. Phys. Soc. (London) **84**, 89 (1964).
[24] Dž. Belkić, R. Gayet, and A. Salin, Phys. Rep. **56**, 279 (1979).
[25] K. R. Greider and L. D. Dodd, Phys. Rev. **146**, 671 (1966); L. D. Dodd and K. R. Greider, *ibid*. **146**, 675 (1966).
[26] D. S. F. Crothers, Nucl. Instrum. Methods Res. Sect. B **27**, 555 (1987).
[27] Dž. Belkić, J. Phys. B **26**, 497 (1993); Phys. Rev. A **47**, 189 (1993).
[28] H. A. Bethe and E. E. Salpeter, *Quantum Mechanics of One- and Two-Electron Atoms* (Springer-Verlag, Berlin, 1957), Chap. 8, p. 37.
[29] L. H. Vainshtein, L. P. Presnyakov, and I. I. Sobel'man, Zh. Eksp. Teor. Fiz. **43**, 518 (1962) [Sov. Phys. JETP **18**, 1383 (1964)].
[30] J. D. Dollard, Ph.D thesis, University of Michigan, 1963 (unpublished); J. Math. Phys. **5**, 729 (1964).
[31] V. Mergel, R. Dörner, M. Achler, Kh. Khayyat, S. Lencinas, J. Euler, O. Jagutzki, S. Nüttgens, M. Unverzagt, L. Spielberger, W. Wu, R. Ali, J. Ullrich, H. Cederquist, A. Salin, R. E. Olson, Dž. Belkić, C. L. Cocke, and H. Schmidt-Böcking, Phys. Rev. Lett. (to be published).
[32] L. H. Thomas, Proc. R. Soc. (London) **114**, 561 (1927).
[33] J. S. Briggs and K. Taulbjerg, J. Phys. B **12**, 2565 (1979); T. Ishihara and J. H. McGuire, Phys. Rev. A **38**, 3310 (1988).
[34] R. Gayet and A. Salin, in *High-Energy Ion-Atom Collisions*, edited by D. Berenyi and G. Hock, Lecture Notes in Physics Vol. 376 (Springer-Verlag, Berlin, 1990), p. 122; J. Phys. B **20**, L571 (1987).
[35] C. L. Cocke and R. E. Olson, Phys. Rep. **205**, 153 (1991).
[36] J. Ullrich, R. Dörner, V. Mergel, O. Jagutzki, L. Spielberger, and H. Schmidt-Böcking, Commun. At. Mol. Phys. **30**, 285 (1994); V. Mergel, R. Dörner, J. Ullrich, O. Jagutzki, S. Lencinas, S. Nüttgens, L. Spielberger, M. Unverzagt, C. L. Cocke, R. E. Olson, M. Schulz, U. Buck, E. Zanger, W. Theisinger, M. Isser, S. Geis, and H. Schmidt-Böcking, Phys. Rev. Lett. **74**, 2200 (1995).
[37] M. Barat and P. Roncin, J. Phys. B **25**, 2205 (1992); J. T. Park, Adv. At. Mol. Phys. **19**, 67 (1983); R. Schuch, H. Schöne, P. D. Miller, H. F. Krause, P. F. Dittner, S. Datz, and R. E. Olson, Phys. Rev. Lett. **60**, 925 (1988).
[38] E. Horsdal-Pedersen, C. L. Cocke, and M. Stockli, Phys. Rev. Lett. **50**, 1910 (1983); J. H. McGuire, M. Stockli, C. L. Cocke, E. Horsdal-Pedersen, and N. C. Sil, Phys. Rev. A **30**, 89 (1984).
[39] H. Vogt, R. Schuch, E. Justiniano, M. Schulz, and W. Schwab, Phys. Rev. Lett. **57**, 2256 (1986).
[40] Dž. Belkić (unpublished).
[41] H.-P. Hülskötter, W. E. Meyerhof, E. A. Dillard, and N. Guardala, Phys. Rev. Lett. **63**, 1938 (1989); J. H. McGuire, N. Stolterfoht, and P. R. Simony, *ibid*. **24**, 97 (1981).
[42] K. L. Wong, W. Wu, E. C. Montenegro, I. Ben-Itzhak, C. L. Cocke, J. P. Giese, and P. Richard, J. Phys. B **29**, L209 (1996).
[43] Dž. Belkić (unpublished).
[44] C. L. Pekeris, Phys. Rev. **112**, 1649 (1958); **115**, 1216 (1959).
[45] A. Nordsieck, Phys. Rev. **93**, 785 (1954).
[46] Dž. Belkić, Phys. Rev. A **37**, 55 (1988).
[47] R. A. Boham and D. A. Kohl, J. Chem. Phys. **45**, 2471 (1966).
[48] C. Eckart, Phys. Rev. **36**, 878 (1930); J. N. Silverman, O. Platas, and F. A. Matsen, J. Chem. Phys. **32**, 1402 (1960).